CD36 promotes chemotherapy resistance and stemness of cervical cancer cells through Hippo and ERK5 pathway activation

Journal:	*SAGE Open Medicine*
Manuscript ID	SOM-25-0830
Manuscript Type:	Original Research Article
Date Submitted by the Author:	30-Jun-2025

Complete List of Authors:	Xie, Linying; The Eighth Affiliated Hospital of Sun Yat-Sen University, Pathology Chen, Zigui; Shenzhen Luohu Hospital Group Luohu People's Hospital, Pathology Xiang, Yali; The Eighth Affiliated Hospital of Sun Yat-Sen University, Pathology Zeng, Chao ; The Eighth Affiliated Hospital of Sun Yat-Sen University, Pathology

Keywords:	CD36, Stemness
Additional Keywords:	Cervical cancer, Chemotherapy resistance

Abstract:	Our previous work revealed that CD36 accelerates progression of cervical cancer. Here, we elucidate the effects of CD36 in regulating stemness and chemotherapy resistance of cervical cancer cells. We used bioinformatics analysis to assess the correlation between CD36 expression and chemotherapy drugs sensitivity in advanced cervical cancer. The effects of CD36 expression on proliferation of cervical cancer cells were analyzed using the CCK8 and colony formation assay. The stemness of cervical cancer cells were assessed by tumorsphere formation assay. Correlations between CD36 expression and stem cell markers were investigated by Western blot. The roles of CD36 on chemotherapy resistance of cervical cancer cells were evaluated by using colony formation assay, CCK8 assay and flow cytometry. Finally, the molecular mechanisms by which CD36 promotes stemness and chemotherapy resistance of cervical cancer cells were explored through bioinformatics analysis and Western blot. CD36 expression was positively correlated with cisplatin resistance in advanced cervical cancer. CD36 overexpression promoted the stemness and chemotherapy resistance of cervical cancer cells. Most importantly, we discovered that CD44, Hippo and MEK5/ERK5 pathways might be involved in CD36-mediated chemotherapy resistance and stemness of cervical cancer cells. CD36 may be an effective therapeutic target for improving the prognosis of cervical cancer.

CD36 promotes chemotherapy resistance and stemness of cervical cancer cells through Hippo and ERK5 pathway activation

Lin-Ying Xie[1,#], Zi-Gui Chen[2,3,#], Ya-Li Xiang[1], Chao Zeng[1,*]

[1]Department of Pathology, The Eighth Affiliated Hospital, Sun Yat-sen University, Shenzhen 518033, China

[2]Department of Pathology, Shenzhen Luohu Hospital of Traditional Chinese Medicine, Shenzhen, 518001, China

[3]Department of Pathology, Shenzhen Hospital Shanghai University of Traditional Chinese Medicine, Shenzhen, 518001, China

[#]Contributed equally to this work.

* Corresponding author: Chao Zeng, Department of Pathology, The Eighth Affiliated Hospital, Sun Yat-sen University, No. 3025 Shennan Middle Road, Futian District, Shenzhen 518033, China. Email: zengch35@mail.sysu.edu.cn.

Abstract

Objective: Our previous work revealed that CD36 accelerates progression of cervical cancer. Here, we elucidate the effects of CD36 in regulating stemness and chemotherapy resistance of cervical cancer cells.

Methods: We used bioinformatics analysis to assess the correlation between CD36 expression and chemotherapy drugs sensitivity in advanced cervical cancer. The effects of CD36 expression on proliferation of cervical cancer cells were analyzed using the CCK8 and colony formation assay. The stemness of cervical cancer cells were assessed by tumorsphere formation assay. Correlations between CD36 expression and stem cell markers were investigated by Western blot. Next, the roles of CD36 on chemotherapy resistance of cervical cancer cells were evaluated by using colony formation assay, CCK8 assay and flow cytometry. Finally, the molecular mechanisms by which CD36 promotes stemness and chemotherapy resistance of cervical cancer cells were explored through bioinformatics analysis and Western blot.

Results: CD36 expression was positively correlated with cisplatin resistance in advanced cervical cancer. CD36 overexpression promoted the stemness and chemotherapy resistance of cervical cancer cells. Most importantly, we discovered that CD44, Hippo and MEK5/ERK5 pathways might be involved in CD36-mediated chemotherapy resistance and stemness of cervical cancer cells.

Conclusions: CD36 may be an effective therapeutic target for improving the prognosis of cervical cancer.

Keywords: CD36; Stemness; Chemotherapy resistance; Cervical cancer

Introduction

Cervical cancer is the most common malignancy of the female genital tract [1]. Its progression involves infection with human papillomavirus, cervical intraepithelial neoplasia, local invasion, and metastasis [2-3]. Widespread use of cytological screening and biopsies has effectively reduced cervical cancer incidence. However, advanced cervical cancer continues to have a poor prognosis due to chemotherapy resistance [4]. Therefore, elucidating the mechanisms underlying chemotherapy resistance in cervical cancer is essential.

Cancer cells utilize fatty acids as an energy source to reprogram metabolism. CD36, a lipid transporter, is a membrane protein expressed on monocytes, epithelial cells, and endothelial cells [5-8]. In cancer cells, CD36 overexpression accelerates fatty acid uptake and lipid accumulation, promoting growth and metastasis [9-12]. Lipid accumulation also exerts immunosuppressive effects [13]. Owing to its multifaceted roles in cancer biology, CD36 has recently emerged as a promising therapeutic target in various cancers [14-18]. Notably, silencing CD36 inhibits clonogenicity and stemness marker expression in bladder cancer cells, highlighting its critical role in enhancing stemness properties [19]. However, current understanding of CD36's role in regulating stemness and chemotherapy resistance in cervical cancer cells remains limited.

Cancer stem cells (CSCs) are tumor-initiating cells that are capable of differentiating into multiple cell types and contributing to tumorigenicity and chemotherapy resistance in solid malignancies [20-22]. However, limited studies have examined the relationship between cervical CSCs, chemotherapy resistance, and cancer progression. CD44, a cervical tumorigenesis stem cell marker, can enhance CSC self-renewal and chemotherapy resistance [23]. Yes-associated protein (YAP) promotes malignant transformation of cervical intraepithelial neoplasia by reinforcing CSC traits [24]. In this study, we explored the roles of CD36 in regulating stemness and chemotherapy resistance in cervical cancer cells. Further, we investigated the specific mechanisms through which CD36 facilitates these processes.

Materials and methods

Acquisition of Cervical Cancer Transcriptome Data

We downloaded transcriptome sequencing data (ribonucleic acid [RNA] sequencing) for cervical cancer from The Cancer Genome Atlas database (https://www.cancer.gov/ccg/research/genome-sequencing/tcga) using the Illumina HiSeq 2000 platform. The dataset included 62 advanced cervical cancer samples (41 stage 4 and 21 additional stage 4 cases). Details of the downloaded data are provided in **Table S1**.

Half-maximal inhibitory concentration (IC50) correlation analysis

CD36 expression levels in cervical cancer specimens from The Cancer Genome Atlas database were analyzed in combination with data from the Genomics of Drug Sensitivity in Cancer database (https://www.cancerrxgene.org/) [25]. The R version 4.3.1 pRRophetic package (https://github.com/paulgeeleher/pRRophetic) was used to evaluate the sensitivity of advanced cervical cancer to various chemotherapeutic agents [26]. Using the downloaded drug data as a reference, the pRRophetic package estimated the IC50 value of each sample based on whole-genome expression.

Kyoto Encyclopedia of Genes and Genomes pathways analysis

The correlation between CD36 gene expression and all of the other genes was calculated in 62 advanced cervical cancer samples using the Pearson correlation coefficient. Genes with correlation coefficients above 0.3 and P-values below 0.05 were retained. The Database for Annotation, Visualization and Integrated Discovery (DAVID) version 6.8 (https://david.ncifcrf.gov/) was then used to perform Kyoto Encyclopedia of Genes and Genomes (KEGG) pathway enrichment analysis on the selected genes, applying a *P*-value threshold of less than 0.05 [27]. There were 10 KEGG pathways that met the significance criteria.

Prognostic analysis

For prognostic analysis, the R version 4.3.1 survival package (version 2.41-1; https://cran.r-project.org/web/packages/finalfit/vignettes/survival.html) was used to evaluate the correlation between CD36 expression and prognosis in advanced cervical cancer [28]. The effects of CD36 expression and clinical stage on patient prognosis were analyzed.

Cell culture

C33a and HeLa cells were obtained from the Type Collection Center (Wuhan, China) and cultured in Dulbecco's Modified Eagle Medium (Gibco, CA, USA). C33a cells were incubated with fluorescein isothiocyanate-labeled CD133 and sorted by flow cytometry. The CD133-positive C33a cell population was collected, expanded, and cultured *in vitro* as C33a-Cervical CSCs (C33a-CCSCs).

Plasmid construction and transfection

The pIRES2-ZsGreen1-CD36 plasmid, designed to overexpress CD36, was constructed by cloning the CD36 coding sequence into the pIRES2-ZsGreen1 vector. C33a-CCSCs were transfected with the plasmid using Lipo™6000 (Beyotime, Shanghai, China) and selected in medium containing 600 μg/ml G418 for three weeks. The empty pIRES2-ZsGreen1-NC plasmid served as a negative control (NC). CD36-overexpressing C33a and C33a-CCSCs cells were designated as “C33a/CD36” and “C33a-CCSCs/CD36,” respectively.

Transfection with siRNA (small interfering RNA)

Human CD36 small interfering ribonucleic acid (siRNA) was purchased from Guangzhou Ribo (Guangzhou, China). Cells were seeded in six-well plates at a density of 2×10^5 cells/well. HeLa cells were transfected with CD36 siRNA (HeLa/siRNA CD36) (sense: 5′-CCUGAUAGAAAUGAUCUUATT-3′; antisense: 5′-UAAGAUCAUUUCUAUCA GGTT-3′) or NC siRNA (HeLa/NC-siRNA) (sense: 5′-UUCUCCGAACGUGUCACGUTT-3′; antisense: 5′-ACGUGACACGUUCGGAG AATT-3′) using Lipo™3000 (Thermo Fisher Scientific, Waltham, USA) at a final concentration of 100 nM.

Flow cytometry analysis of the ratios of CD133 positive cervical cancer cells

C33a/CD36 and HeLa/CD36-siRNA cells were centrifuged at 1500 rpm for 5 min. The cells were resuspended in 200 μl of phosphate-buffered saline, followed by the addition of 5 μl of CD133 antibody to each flow tube. Samples were incubated at 4°C for 30 min. After adding another 200 μl of phosphate-buffered saline, the proportion of CD133-positive cells was analyzed by flow cytometry.

Tumorsphere formation assay

C33a/CD36, C33a-CCSCs/CD36, or HeLa/siRNA CD36 cells were incubated in Dulbecco's Modified Eagle Medium supplemented with 20 ng/ml basic fibroblast growth factor, 20 ng/ml epidermal growth factor, and 1×B27. Cells were seeded in low-attachment six-well plates at a density of 2×10^4 cells/well and cultured for 10 days. Three fields were randomly selected from confocal images, and the number of stem cell spheres with diameters greater than 100 μm was counted for each group.

Western blot

After boiling for 8 min, total protein (80 μg) was loaded onto a 10% polyacrylamide gel and transferred to a polyvinylidene fluoride membrane. The membrane was incubated with the following primary antibodies: CD36 (1:1000; Ab252923, Abcam, Cambridge, UK), CD44 (1:3000; A19020, Abclonal, MA, USA), CD133 (1:1000; AF5120, Affinity, Cincinnati, USA), Nanog (1:5000; 67255-1-Ig, Sanying, Wuhan, China), YAP (1:1000; AF6328, Affinity, Cincinnati, USA), TAZ (1:300; A8202, Abclonal, MA, USA), Bcl-2 (1:3000; 26593-1-AP, Sanying, Wuhan, China), Bax (1:10000; 60627-1-Ig, Sanying, Wuhan, China), MEK5 (1:2000; DF7667, Affinity, Cincinnati, USA), ERK5 (1:1000; DF6835, Affinity, Cincinnati, USA), cleaved caspase-3 (1:1000; AF7022, Affinity, Cincinnati, USA), and GAPDH (1:1000; AB-P-R001, Xianzhi Biology, Hangzhou, China). Membranes were then incubated with horseradish peroxidase-conjugated secondary antibodies (1:10000; BA1051, BA1054; Boster Biology, Wuhan, China). Proteins were visualized using a chemiluminescence kit (Pierce; Thermo Fisher Scientific, Inc., Massachusetts, USA).

Colony formation assay

HeLa/siRNA CD36, HeLa/NC siRNA, and HeLa cells were seeded at 200 cells/well in six-well plates [29]. The cells were incubated at 5% CO_2. After 14 days, colonies were stained with trypan blue, and the number of cell colonies was counted.

CCK8 assay

C33a/CD36, C33a-CCSCs, HeLa/siRNA CD36 cells and the corresponding control groups were inserted into 96-well plates with 5×10^3 cells per well and cultured 24h at 37°C. Add 10μl cck8 per well and culture at 37°C for 2h. The absorbance value OD450 of each well was determined by microplate reader. Cell survival rate %= [(experimental hole absorbance) - (blank hole absorbance)]/[control hole absorbance) - (blank hole absorbance)] ×100%

TUNEL assay

C33a-CCSCs, C33a-CCSCs/CD36 and C33a-CCSCs/NC were seeded at a density of 4×10^5 cells/well in six-well plates. After added 0.5 ml fixative, the cells were permeabilized by 0.2% Triton X-100. Removed the excess PBS, 100 μl of TUNEL equilibrium solution was added to each sample. A TUNEL reaction mixture containing TdT enzyme and fluorescein-dUTP was applied and incubated at 37 °C for 2h. Then diluted DAPI was added, and the samples were further incubated at room temperature for 5 min. The samples were observed under a fluorescence microscope.

Immunofluorescence

After the tissue sections were deparaffinized, antigen repair was performed. After blocking non-specific binding with 5% diluted goat serum, sections were incubated with primary antibodies against CD44 (dilution, 1:100; A19020, Abclonal, MA, USA) and CD133(dilution, 1:100; AF5120, Affinity, Cincinnati, USA) at 4°C overnight, then incubated with secondary antibody (dilution, 1:100; BA1105, BOSTER, Wuhan, China). Nuclei were stained by 4′,6- Diamidino-2-phenylindole (DAPI). After using anti-fluorescence quencher, the images were observed under a fluorescence microscope. Image-Pro Plus 6.0 software (Media Cybernetics,Maryland, USA) was used to quantitatively analyze the expressions of CD133 and CD44 in each group. The mean optical density value represents the protein expression level.

Flow Cytometry analysis of apoptosis

Cells were centrifuged at 1500rpm for 5 min. The ratios of apoptotic in cervical cancer cells were measured using Annexin V FITC/PI Apoptosis Detection Kit.

Animal assay

Four-week-old female BALB/C nude mice were purchased from SiBei Fu Animal Center（Beijing, China）. C33a/CD36 cells (2×10^{6}/mL) were injected subcutaneously into the axillary of right forelimb of nude mice. Each group had six nude mice. In vivo imaging detection was performed with a small animal in vivo imager (IVIS Lumina III, Perkin Elmer). We euthanized the nude mice with anesthesia. The animal experiment protocol was carried out in accordance with the regulations of the Institutional Animal Ethical Care Committee of the Eighth Affiliated Hospital, Sun Yat-sen University（2024r005）.

Statistical analysis

Data are presented as mean ± standard error of the mean (SEM). The overall survival rate was calculated by plotting the survival curve with the Kaplan-Meier method. Statistical comparisons of data from the experiments on cultured cells or mice were performed using the two-tailed Student's *t* test. All of the statistical analyses were performed using Statistical Package for the Social Sciences version 17.0 (SPSS Inc., Chicago, USA). Differences were considered significant when the p value was less than 0.05.

Results

Correlation between CD36 expression level and resistance of chemotherapy drugs in advanced cervical cancer.

The IC50 value reflects the sensitivity of chemotherapeutic drugs, and its correlation with CD36 expression was evaluated through bioinformatics analysis (**Table S2**). Notably, higher CD36 expression in advanced cervical cancer was associated with increased IC50 values for cisplatin. Additionally, CD36 expression showed a positive correlation with cisplatin resistance and a negative correlation with vinorelbine resistance in advanced cervical cancer (**Figure 1A**).

Analysis of downstream pathways regulated by CD36 in advanced cervical cancer

In 62 advanced cervical cancer samples, 648 genes were identified as significantly associated with CD36 expression (**Table S3**). KEGG pathway enrichment analysis was conducted using DAVID version 6.8. There were 10 KEGG pathways that were identified based on a P-value threshold of < 0.05 (**Figure 1B).** Among these, the Hippo and MEK5/ERK5 signaling pathways were associated with chemotherapy resistance and cancer cell stemness. However, no correlation was observed between CD36 expression and prognosis in patients with advanced cervical cancer (**Figure 1C–F**). CD36 expression was positively correlated with the expression of CD44, CD133, YAP, TAZ, MEK5, and ERK5 in cervical cancer cells (**Figure 1G–J**). These results suggest that CD36 may enhance stem cell marker expression and activate the Hippo and MEK5/ERK5 pathways *in vitro*.

CD36 promotes stemness and tumor growth in vivo

After six weeks, CD36 overexpression significantly promoted tumor growth in female BALB/c-nu mice compared with the C33a/Con group (1636.12 ± 462.29 mm³ verses 732.64 ± 329.89 mm³; **Figure 2A–C**). Additionally, immunofluorescence assays showed that CD133 (mean optical density: 0.81 ± 0.04 vs. 0.31 ± 0.01; **Figure 2D**) and CD44 expression (0.95 ± 0.05 vs. 0.48 ± 0.03; **Figure 2E**) were increased in the C33a/CD36 group compared with controls. These findings suggest that CD36 may promote cervical cancer cell growth by enhancing stemness *in vivo*.

CD36 promoted the stemness of cervical cancer cells in vitro

As shown in **Figure 3A–B**, the number of stem cell spheres with diameters greater than 100 μm was higher in the C33a/CD36 group (5.33 ± 0.58) than in the C33a/NC group (1.67 ± 0.58) and C33a group (2.33 ± 0.57). The Cell Counting Kit-8 assay revealed that CD36 overexpression significantly enhanced the proliferative capacity of C33a cells (**Figure 3D**). In contrast, the number of spheres larger than 100 μm decreased in the HeLa/siRNA CD36 group (2.33 ± 0.58) compared with the HeLa/NC-siRNA group (5.33 ± 0.57) and HeLa group (4.34 ± 0.54) (**Figure 3A, C**). Proliferation was also reduced in the HeLa/siRNA CD36 group relative to the HeLa/NC-siRNA and HeLa groups (**Figure 3E**). Flow cytometry analysis further demonstrated a higher percentage of CD133-positive cells in the C33a/CD36 group (8.35 ± 0.30%) than in the C33a/NC group (3.45 ± 0.21%) and C33a group (3.33 ± 0.37%) (Figure 3F, H). Conversely, fewer CD133-positive cells were observed in the HeLa/siRNA CD36 group (2.44 ± 0.33%) compared with the HeLa/NC-siRNA (5.07 ± 0.11%) and HeLa groups (5.06 ± 0.52%) (**Figure 3G and I**). These findings suggest that CD36 plays a critical role in promoting the stemness of cervical cancer cells *in vitro*.

CD36 overexpression augmented stemness of cervical CSCs

We further sorted CD133-positive C33a cells using flow cytometry and established a CD36-overexpressing cervical cancer stem cell model (C33a-CCSCs/CD36) along with a corresponding control group (C33a-CCSCs/NC). Western blot analysis confirmed that CD36 expression was successfully upregulated in the C33a-CCSCs/CD36 group (**Figure 4A and D**). The number of stem cell spheres with diameters exceeding 100 μm was significantly higher in the C33a-CCSCs/CD36 group (7.33 ± 0.58) than in the C33a-CCSCs/NC group (3.67 ± 0.58) and the C33a-CCSCs group (3.33 ± 0.57) (**Figure 4B**). Similarly, the proliferative capacity of the C33a-CCSCs/CD36 group was markedly elevated compared with both control groups (**Figure 4C**). Immunofluorescence assays also showed increased CD44 expression in the C33a-CCSCs/CD36 group relative to the C33a-CCSCs/NC group (**Figure 4E**). These findings suggest that CD36 overexpression may enhance the stemness of cervical CSCs.

Elevating CD36 expression potentiated the chemotherapy resistance of cervical CSCs through Hippo and MEK5/ERK5 pathways activation.

To further assess whether CD36 expression influences chemotherapy resistance in cervical CSCs, C33a-CCSCs/CD36, C33a-CCSCs/NC, and C33a-CCSCs were treated with 20 μg/ml cisplatin for 24 h. As depicted in **Figure 5A**, the C33a-CCSCs/CD36 group exhibited higher proliferative capacity (130.98 ± 3.15%) compared with the C33a-CCSCs/NC group (97.89 ± 1.28%) and the C33a-CCSCs group (99.57 ± 0.54%). Additionally, the C33a-CCSCs/CD36 group displayed the fewest apoptotic cells relative to the control groups (**Figure 5F**). The expression levels of YAP, TAZ, MEK5, and ERK5 were also elevated in the C33a-CCSCs/CD36 group compared with the controls (**Figure 5D-E**).

To further investigate whether the Hippo and MEK5/ERK5 pathways contribute to CD36-regulated chemotherapy resistance in cervical CSCs, C33a-CCSCs/CD36 cells were treated with Verteporfin (a YAP inhibitor) and XMD8-92 (an ERK5 inhibitor). As shown in **Figure 5B-C**, proliferative capacity decreased following treatment with Verteporfin (117.13 ± 1.78% vs. 99.14 ± 0.84%; 99.18 ± 0.47%) or XMD8-92 (120.99 ± 2.32% vs. 99.37 ± 0.74%; 98.43 ± 0.92%) compared with the C33a-CCSCs + cisplatin and C33a-CCSCs/NC+cisplatin groups. Additionally, the number of apoptotic cells in the C33a-CCSCs/CD36 group increased relative to controls after treatment with either inhibitor (**Figure 5G, H**). These findings indicate that CD36 may induce chemotherapy resistance in cervical CSCs via activation of the Hippo and MEK5/ERK5 pathways.

Interfering CD36 expression alleviated the chemotherapy resistance of cervical cancer cells

Conversely, we downregulated CD36 expression in HeLa cells and treated them with 20 μg/ml cisplatin for 24 hours. The colony formation assay revealed fewer colonies in the HeLa/siRNA CD36 group (106.67 ± 14.57) compared with the HeLa/NC siRNA group (161.33 ± 8.08) and HeLa group (148.33 ± 10.02) (**Figure 6A**). The proliferative capacity of the HeLa/siRNA CD36 group (75.10 ± 3.12%) was significantly reduced relative to the HeLa group (94.15 ± 1.18%) and HeLa/ NC-siRNA group (97.48 ± 2.57%) (**Figure 6B**). The HeLa/siRNA CD36 group also exhibited the highest number of apoptotic cells (35.28 ± 1.15% vs. 21.27 ± 0.88%; 21.26 ± 0.67%) (**Figure 6C, E**). Furthermore, Bcl-2 expression was decreased, Bax expression increased, and cleaved caspase-3 activity enhanced in the HeLa/siRNA CD36 group, consistent with CD36 downregulation (**Figures 6D, F**). These findings indicate that silencing CD36 inhibits proliferation and promotes apoptosis in HeLa cells following cisplatin treatment. Additionally, the expression of CD44, CD133, and Nanog was significantly reduced in the HeLa/siRNA CD36 group compared with controls (**Figure 6D, F**), suggesting that CD36 knockdown may alleviate chemotherapy resistance by suppressing cervical cancer cell stemness.

Discussion

Previous studies have shown that CD36 promotes the progression and metastasis of oral cancer by facilitating the uptake of exogenous fatty acids [11]. Our prior work also demonstrated that CD36 accelerates epithelial-mesenchymal transition and metastasis in cervical cancer [30]. Additionally, CD36-driven lipid uptake contributes to chemotherapy resistance. In acute myeloid leukemia, the CD36–fatty acid oxidation (FAO)–oxidative phosphorylation (OXPHOS) axis underlies resistance to chemotherapy [31]. In this study, we investigated the roles of CD36 in regulating stemness and chemotherapy resistance in cervical cancer cells.

In our study, we found that CD36 promoted the formation of larger stem cell spheres and enhanced the expression of stem cell markers. Additionally, both the proliferative capacity and sphere-forming ability increased following CD36 transfection in C33a-CCSCs. Similarly, Gyamfi et al. reported that CD36 knockdown reduced stemness marker expression in breast cancer cells [32]. Collectively, our results demonstrate that CD36 promotes the stemness of cervical cancer cells.

Chemotherapy resistance is a major factor limiting the clinical efficacy of cervical cancer treatment. Bioinformatics analysis revealed that CD36 expression was positively correlated with cisplatin resistance in advanced cervical cancer. Therefore, we investigated the role of CD36 in chemotherapy resistance. CD36 overexpression enhanced proliferation and reduced apoptosis in C33a-CCSCs treated with cisplatin. In contrast, CD36 silencing decreased colony formation and proliferation in HeLa cells while increasing apoptosis. These findings suggest that CD36 plays a key role in promoting chemotherapy resistance in cervical cancer cells.

CD44 is a well-established cancer stem cell marker and a key regulator of epithelial–mesenchymal transition [33]. We found that CD36 enhances CD44 expression both *in vitro* and *in vivo*, thereby promoting the stemness of cervical cancer cells. The ERK5 and Hippo pathways are also recognized as important contributors to chemotherapy resistance and stemness in cancer cells [34-37]. YAP, a central effector of the Hippo pathway, promotes immune evasion in BRAF inhibitor-resistant melanoma by upregulating PD-L1 [38], while the MEK5–ERK5 –STAT3 axis accelerates self-renewal and tumorigenicity in glioma stem cells [39]. In our study, CD36 upregulated the expression of YAP, TAZ, MEK5, and ERK5, thereby activating both the Hippo and ERK5 pathways. Vittoria et al. reported that Hippo pathway activation is mediated through mitogen-activated protein kinase (MAPK) signaling [40], and CD36 has been shown to activate MAPK signaling [41]. Thus, we speculate that CD36 may activate the Hippo pathway via MAPK activation. Moreover, treatment with YAP and ERK5 inhibitors reduced proliferation and increased apoptosis in C33a-CCSCs/CD36 cells, further supporting the involvement of the Hippo and ERK5 pathways in CD36-mediated chemotherapy resistance.

Conclusion

In summary, our findings demonstrate that CD36 promotes stemness and chemotherapy resistance in cervical cancer cells. Notably, CD44, Hippo, and MEK5/ERK5 pathways are involved in CD36-mediated resistance and contribute to enhanced stemness. Collectively, these results suggest that CD36 may serve as a promising therapeutic target for improving the prognosis of cervical cancer.

Declaration of conflicting interests

The authors declare that they have no conflicts of interest.

Funding

This project was funded by a grant from Shenzhen Science and Technology Program (JCYJ20220530144407017) and Guangdong Provincial Basic and Applied Basic Research Foundation Project (2025A1515011028) .

Supplemental material

The supplemental material for this article is available online.

References

1. Arbyn M, Weiderpass E, Bruni L, et al. Estimates of incidence and mortality of cervical cancer in 2018: A worldwide analysis. *Lancet Glob Health* 2020; 8:191-203.

2. Wu P, Xiong H, Yang M, et al. Co-infections of HPV16/18 with other high-risk HPV types and the risk of cervical carcinogenesis: A large population-based study. *Gynecol Oncol* 2019; 155: 436-443.

3. Sundström K, Eloranta S, Sparén P, et al. Prospective study of human papillomavirus (HPV) types, HPV persistence, and risk of squamous cell carcinoma of the cervix. *Cancer Epidemiol Biomarkers Prev* 2010; 19: 2469-2478.

4. Ferrandina G, Lauriola L, Distefano MG, et al. Increased cyclooxygenase-2 expression is associated with chemotherapy resistance and poor survival in cervical cancer patients. *J Clin Oncol* 2002; 20: 973-981.

5. Martin C, Chevrot M, Poirier H, et al. CD36 as a lipid sensor. *Physiol Behav* 2011;105: 336-342.

6. Hale JS, Otvos B, Sinyuk M. Cancer stem cell-specifc scavenger receptor CD36 drives glioblastoma progression. *Stem Cells* 2014; 32: 1746-1758.

7. Zhao J, Zhi Z, Wang C, et al.Exogenous lipids promote the growth of breast cancer cells via CD36. *Oncol Rep* 2017; 38: 2105-2115.

8. Zhou X, Su M, Lu J, et al. CD36: The Bridge between lipids and tumors. *Molecules* 2024; 29: 531.

9. Ladanyi A, Mukherjee A, Kenny HA, et al. Adipocyte-induced CD36 expression drives ovarian cancer progression and metastasis. *Oncogene* 2018; 37: 2285-2301.

10. Liu H, Guo W, Wang T, et al. CD36 inhibition reduces non-small-cell lung cancer development through AKT-mTOR pathway. *Cell Biol Toxicol* 2024; 40: 10.

11. Pascual G, Avgustinova A, Mejetta S, et al. Targeting metastasis-initiating cells through the fatty acid receptor CD36. *Nature* 2017; 541: 41-45.

12. Wang H, Liu F, Wu X, et al. Cancer-associated fibroblasts contributed to hepatocellular carcinoma recurrence and metastasis via CD36-mediated fatty-acid metabolic reprogramming. *Exp Cell Res* 2024;435: 113947.

13. Zhu GQ, Tang Z, Huang R, et al. CD36$^+$ cancer-associated fibroblasts provide immunosuppressive microenvironment for hepatocellular carcinoma via secretion of macrophage migration inhibitory factor. *Cell Discov.* 2023; 9: 25.

14. Liao M, Li Y, Xiao A, et al. HIF-2α-induced upregulation of CD36 promotes the development of CCRCC. *Exp Cell Res 2022;* 421: 113389.

15. Liu LZ, Wang B, Zhang R, et al.The activated CD36-Src axis promotes lung adenocarcinoma cell proliferation and actin remodeling-involved metastasis in high-fat environment. *Cell Death Dis* 2023; 14:548.

16. Luo X, Zheng E, Wei L, et al. The fatty acid receptor CD36 promotes HCC progression through activating Src/PI3K/AKT axis-dependent aerobic glycolysis. *Cell Death Dis* 2021; 12: 328.

17. Pan J, Fan Z, Wang Z, et al. CD36 mediates palmitate acid-induced metastasis of gastric cancer via AKT/GSK-3β/β-catenin pathway. *J Exp Clin Cancer Res* 2019; 38: 52.

18. Tao L, Ding X, Yan L, et al. CD36 accelerates the progression of hepatocellular carcinoma by promoting FAs absorption. *Med Oncol* 2022; 39: 202.

19. Yang L, Sun J, Li M, et al. Oxidized low-density lipoprotein links hypercholestero -lemia and bladder cancer aggressiveness by promoting cancer stemness. *Cancer Res* 2021; 81: 5720-5732.

20. Bao S, Wu Q, McLendon RE. Glioma stem cells promote radioresistance by preferential activation of the DNA damage response. *Nature* 2006; 444: 756-760.

21. Lopez-Ayllon BD, Moncho-Amor V, Abarrategi A. Cancer stem cells and cisplatin-

resistant cells isolated from non-small-lung cancer cell lines constitute related cell populations. *Cancer Med* 2014; 3: 1099-1111.

22. Srivastava AK, Han C, Zhao R,et al. Enhanced expression of DNA polymerase eta contributes to cisplatin resistance of ovarian cancer stem cells. *Proc Natl Acad Sci USA* 2015; 112: 4411-4416.

23. Zhang J, Chen X, Bian L, et al. $CD44^{+}/CD24^{+}$-expressing cervical cancer cells and radioresistant cervical cancer cells exhibit cancer stem cell characteristics. Gynecol *Obstet Invest* 2019; 84:174-182.

24. Li S, Li X, Yang YB, et al. YAP/TAZ-TEAD activity promotes the malignant transformation of cervical intraepithelial neoplasia through enhancing the characteristics and Warburg effect of cancer stem cells. *Apoptosis* 2024; 29: 1198-1210.

25. Yang W, Soares J, Greninger P, et al. Genomics of Drug Sensitivity in Cancer: a resource for therapeutic biomarker discovery in cancer cells. *Nucleic Acids Res.* 2013; 41: 955-961.

26. Zhu Y, Meng X, Ruan X, et al. Characterization of neoantigen load subgroups in gynecologic and breast cancers. *Front Bioeng Biote*chnol 2020; 13: 702.

27. Huang daW, Sherman BT, Lempicki RA. Systematic and integrative analysis of large gene lists using DAVID bioinformatics resources. *Nat Protoc* 2009; 4: 44-57.

28. Wang P, Wang Y, Hang B, et al. A novel gene expression-based prognostic scoring system to predict survival in gastric cancer. *Oncotarget* 2016; 7: 55343-55351.

29. Zeng C, Ke Z, Song Y, et al. Annexin A3 is associated with a poor prognosis in breast cancer and participates in the modulation of apoptosis in vitro by affecting the Bcl-2/Bax balance. *Exp Mol Pathol* 2013; 95: 23-31.

30. Deng M, Cai X, Long L, et al. CD36 promotes the epithelial-mesenchymal transition and metastasis in cervical cancer by interacting with TGF-beta. *J Transl Med* 2019; 17: 352.

31. Farge T, Saland Estelle, Toni Fde, et al. Chemotherapy-resistant human acute myeloid leukemia cells are not enriched for leukemic stem cells but require oxidative metabolism. *Cancer Discov* 2017; 7: 716-735.

32. Gyamfi J, Yeo JH, Kwon D, et al. Interaction between CD36 and FABP4 modulates adipocyte-induced fatty acid import and metabolism in breast cancer. *NPJ Breast Cancer* 2021; 7: 129.

33. Fukasawa K, Lyu J, Kubo T, et al. MEK5-ERK5 axis promotes self-renewal and tumorigenicity of glioma stem cells. *Cancer Res Commun* 2023; 3: 148-159.

34. Pereira DM, Gomes SE, Borralho PM, et al. MEK5 /ERK5 activation regulates colon cancer stem-like cell properties. *Cell Death Discov* 2019; 5: 68.

35. Song R, Gu D, Zhang L, et al. Functional significance of Hippo/YAP signaling for drug resistance in colorectal cancer. *Mol Carcinog* 2018; 57:1608-1615.

36. Sa P, Singh P, Panda S, et al. Reversal of cisplatin resistance in oral squamous cell carcinoma by piperlongumine loaded smart nanoparticles through inhibition of Hippo-YAP signaling pathway. *Transl Res* 2024; 268: 63-78.

37. Lambrescu IM, Gaina GF, Ceafalan LC, et al. Inside anticancer therapy resistance

and metastasis. Focus on CD36. *J Cancer* 2024; 15: 1675-1686.

38. Chan NY, Yi Cl.YAP/TAZ Signaling and resistance to cancer therapy. *Trends Cancer* 2019; 5: 283-296.

39. Fukasawa K, Lyu J, Kubo T, et al. MEK5-ERK5 axis promotes self-renewal and tumorigenicity of glioma stem cells. Cancer Res Commun 2023; 3:148-159.

40. Vittoria MA, Kingston N, Kotynkova K, et al.Inactivation of the Hippo tumor suppressor pathway promotes melanoma. Nat Commun. 2022; 13: 3732.

41. Nan P, Dong X, Bai X, et al. Tumor-stroma TGF-β1-THBS2 feedback circuit drives pancreatic ductal adenocarcinoma progression via integrin αvβ3/CD36-mediated activation of the MAPK pathway. *Cancer Lett* 2022; 528:59-75.

Figure Legend

Figure 1. Correlation between CD36 expression and resistance of chemotherapy drugs and prognosis of cervical cancer and its regulated signaling pathways. A: CD36 expression had the most significant positive correlation with cisplatin resistance and the most significant negative correlation with vinorelbine in advanced cervical cancer by IC50 correlation analysis. Scale represents P value. B:KEGG analysis downstream pathways regulated by CD36 in advanced cervical cancer. C: Kaplan-Meier analysis showed the prognosis of stage 3 cervical cancer was significantly better than stage 4 cervical cancer. D: Kaplan-Meier analysis showed CD36 expression was not correlated with the prognosis of advanced cervical cancer. E: Kaplan-Meier analysis showed CD36 expression was not correlated with the prognosis of cervical cancer in stage 3. F: Kaplan-Meier analysis showed CD36 expression was not correlated with the prognosis of cervical cancer in stage 4. G, I: The expressions of CD44, CD133, Nanog, YAP, TAZ, MEK5 and ERK5 were increased after enhanced CD36 expression in C33a cells. H.J: The expressions of CD44, CD133, Nanog, YAP, TAZ, MEK5 and ERK5 in HeLa cells were reduced along with the down-regulation of CD36.

Figure 2. CD36 promotes stemness and tumor growth. A: CD36 over-expression (C33a/CD36 group) promoted tumor growth in vivo compared with the control group (C33a/Con group). B: The upper row: C33a /CD36 group; The bottom row: C33a/Con

group. C: Statistical plots of tumor volume in C33a/CD36 group and C33a/Con group (n=6). D: CD133 expression in C33a/CD36 group was significantly enhanced compared with the C33a/Con group（×400）. E: CD44 expression in C33a/CD36 group was significantly enhanced compared with the C33a/Con group (×400).

Figure 3. CD36 promotes stemness of cervical cancer cells. A, B. The number of stem cell spheres with a diameter larger than 100μm in C33a/CD36 group was the highest. A-C: Interfering with CD36 expression in HeLa cells suppressed the number of stem cell spheres larger than 100μm (A:×200). D: The proliferative ability of C33a/CD36 group was increased compared with the C33a and C33a/NC group. E: Interfering with CD36 expression suppressed the proliferative ability of HeLa cells. F: The CD133-positive cells in the C33a/CD36 group were the highest compared with the C33a and C33a/NC group. G. The CD133-positive cells in the HeLa/siRNA CD36 group were the least compared with the HeLa and HeLa/NC siRNA group. H.Statistical chart of CD133-positive cell rate in C33a, C33a/NC and C33a/CD36 group. I. Statistical chart of CD133-positive cell rate in HeLa, HeLa/NC siRNA and HeLa/siRNA CD36 group. All experiments were performed in triplicate.**P*<0.05.

Figure 4. Effect of CD36 overexpression on stemness of cervical cancer stem cells. A, D: Compared with C33a-CCSCs and C33a-CCSCs/NC, CD36 expression was significantly enhanced in the C33a-CCSCs/CD36 group. B: The number of stem cell spheres with a diameter larger than 100μm in C33a-CCSCs/CD36 group was the highest compared with the C33a-CCSCs and C33a-CCSCs/NC group (B:×200). C: The proliferative ability of C33a-CCSCs/CD36 group was increased compared with the C33a-CCSCs and C33a-CCSCs/NC group. E: CD44 expression was increased in C33a-CCSCs/CD36 group compared with C33a-CCSCs/NC group (E:×400). **P*<0.05.

Figure 5. The effects of CD36 expression on chemotherapy resistance of cervical cancer stem cells. A: CD36 promotes proliferative ability of C33a-CCSCs. B,C: Verteporfin and XMD8-92 inhibited proliferation of C33a-CCSCs to some extent. D,E: CD36 increased the the expression levels of YAP, TAZ and ERK5. F: CD36 inhibited apoptosis of C33a-CCSCs. G: Verteporfin promotes apoptosis of C33a-CCSCs. H: XMD8-92 promotes apoptosis of C33a-CCSCs. All experiments were performed in triplicate. **P*<0.05.

Figure 6. Effects of interfering CD36 expression on chemotherapy resistance of Hela cells. A: Interfering CD36 expression inhibited clone formation ability of HeLa cells after treated with cisplatin. B: Interfering CD36 expression inhibited proliferative ability of HeLa cells after treated with cisplatin. C, E: Interfering CD36 expression promoted apoptosis of HeLa cells after treated with cisplatin. D, F: Compared with the control groups, expression of CD44, CD133, Nanog, Bcl-2 were decreased and expression of Bax, Caspase-3 were increased in the HeLa/siRNA CD36 group. All experiments were performed in triplicate.**P*<0.05.

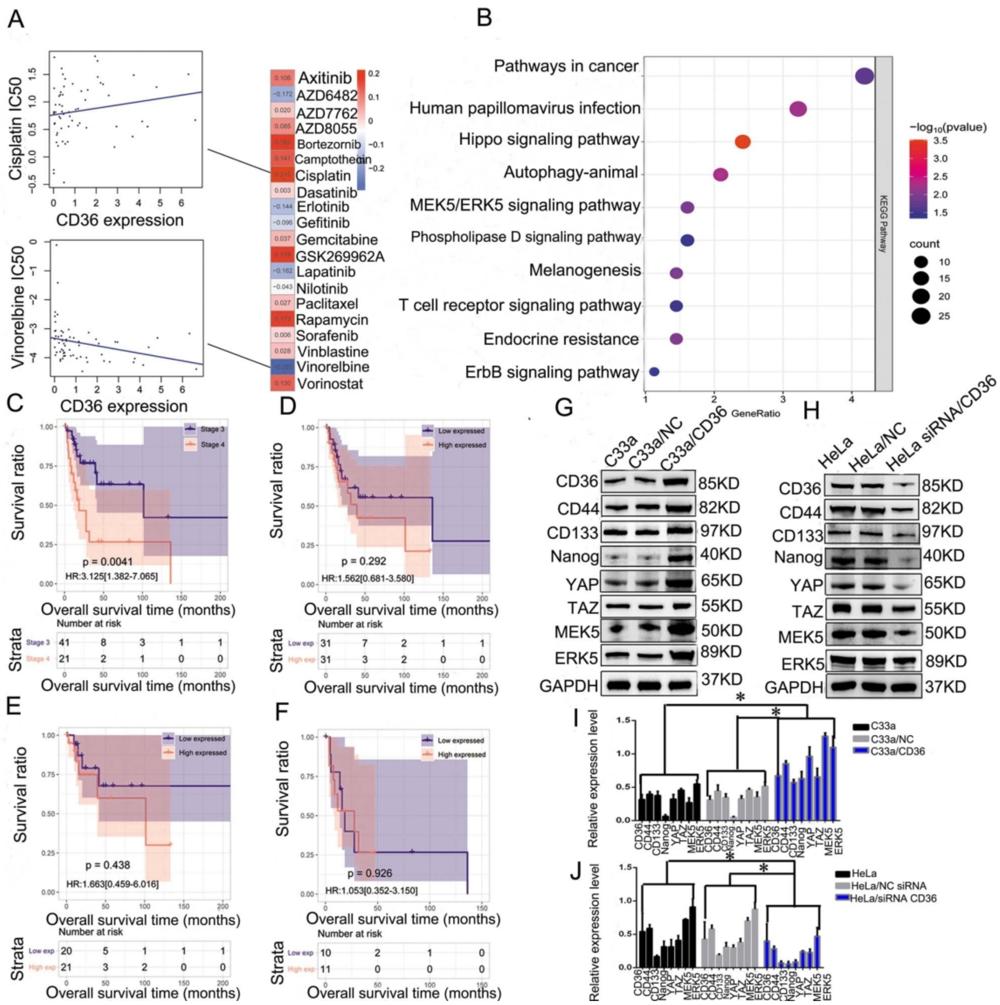

Figure 1. Correlation between CD36 expression and resistance of chemotherapy drugs and prognosis of cervical cancer and its regulated signaling pathways. A: CD36 expression had the most significant positive correlation with cisplatin resistance and the most significant negative correlation with vinorelbine in advanced cervical cancer by IC50 correlation analysis. Scale represents P value. B:KEGG analysis downstream pathways regulated by CD36 in advanced cervical cancer. C: Kaplan-Meier analysis showed the prognosis of stage 3 cervical cancer was significantly better than stage 4 cervical cancer. D: Kaplan-Meier analysis showed CD36 expression was not correlated with the prognosis of advanced cervical cancer. E: Kaplan-Meier analysis showed CD36 expression was not correlated with the prognosis of cervical cancer in stage 3. F: Kaplan-Meier analysis showed CD36 expression was not correlated with the prognosis of cervical cancer in stage 4. G, I: The expressions of CD44, CD133, Nanog, YAP, TAZ, MEK5 and ERK5 were increased after enhanced CD36 expression in C33a cells. H.J: The expressions of CD44, CD133, Nanog, YAP, TAZ, MEK5 and ERK5 in HeLa cells were reduced along with the down-regulation of CD36.

169x169mm (300 x 300 DPI)

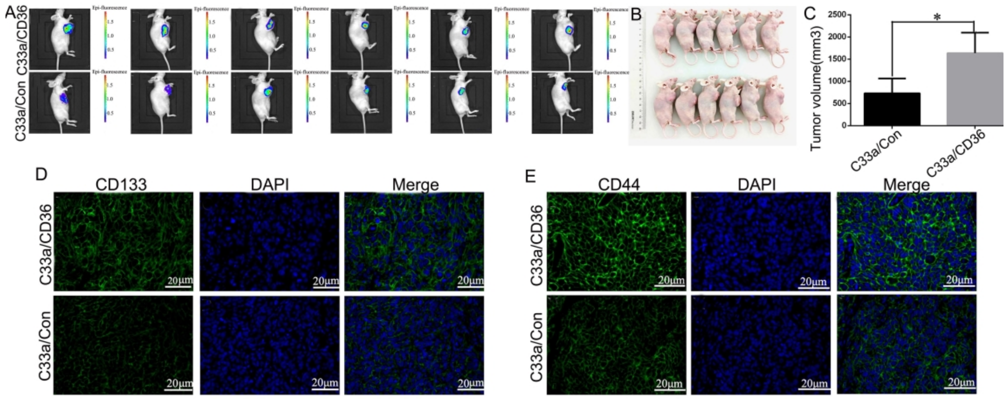

Figure 2. CD36 promotes stemness and tumor growth. A: CD36 over-expression (C33a/CD36 group) promoted tumor growth in vivo compared with the control group (C33a/Con group). B: The upper row: C33a /CD36 group; The bottom row: C33a/Con group. C: Statistical plots of tumor volume in C33a/CD36 group and C33a/Con group (n=6). D: CD133 expression in C33a/CD36 group was significantly enhanced compared with the C33a/Con group（×400）. E: CD44 expression in C33a/CD36 group was significantly enhanced compared with the C33a/Con group (×400).

338x134mm (300 x 300 DPI)

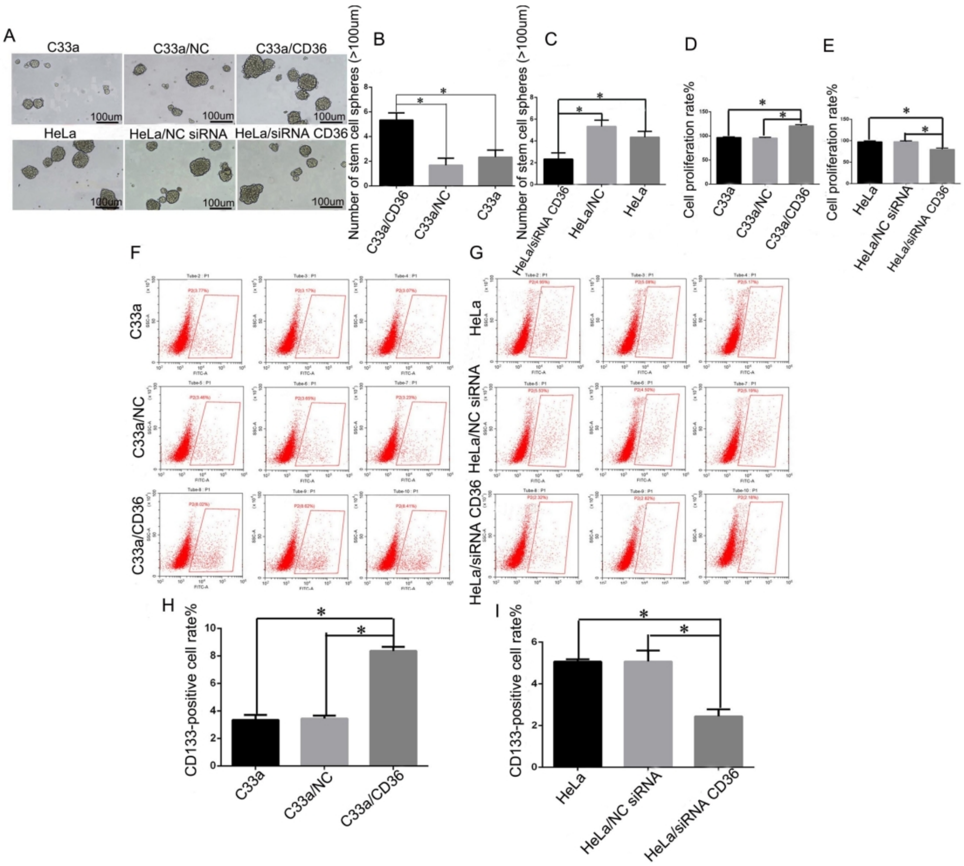

Figure 3. CD36 promotes stemness of cervical cancer cells. A, B. The number of stem cell spheres with a diameter larger than 100μm in C33a/CD36 group was the highest. A-C: Interfering with CD36 expression in HeLa cells suppressed the number of stem cell spheres larger than 100μm (A:×200). D: The proliferative ability of C33a/CD36 group was increased compared with the C33a and C33a/NC group. E: Interfering with CD36 expression suppressed the proliferative ability of HeLa cells. F: The CD133-positive cells in the C33a/CD36 group were the highest compared with the C33a and C33a/NC group. G. The CD133-positive cells in the HeLa/siRNA CD36 group were the least compared with the HeLa and HeLa/NC siRNA group. H.Statistical chart of CD133-positive cell rate in C33a, C33a/NC and C33a/CD36 group. I. Statistical chart of CD133-positive cell rate in HeLa, HeLa/NC siRNA and HeLa/siRNA CD36 group. All experiments were performed in triplicate.*P<0.05.

233x200mm (300 x 300 DPI)

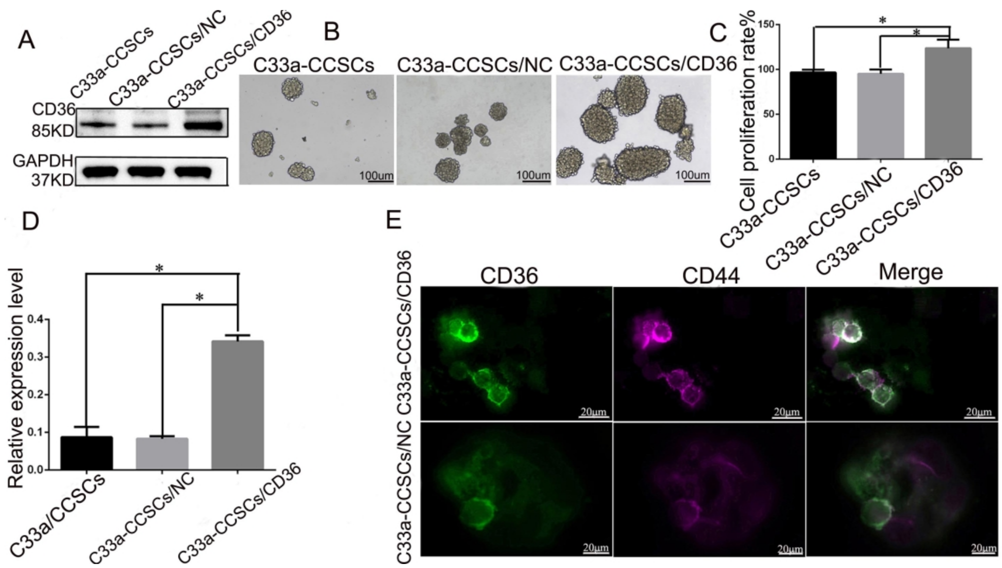

Figure 4. Effect of CD36 overexpression on stemness of cervical cancer stem cells. A, D: Compared with C33a-CCSCs and C33a-CCSCs/NC, CD36 expression was significantly enhanced in the C33a-CCSCs/CD36 group. B: The number of stem cell spheres with a diameter larger than 100μm in C33a-CCSCs/CD36 group was the highest compared with the C33a-CCSCs and C33a-CCSCs/NC group (B:×200). C: The proliferative ability of C33a-CCSCs/CD36 group was increased compared with the C33a-CCSCs and C33a-CCSCs/NC group. E: CD44 expression was increased in C33a-CCSCs/CD36 group compared with C33a-CCSCs/NC group (E:×400). *P<0.05.

246x136mm (300 x 300 DPI)

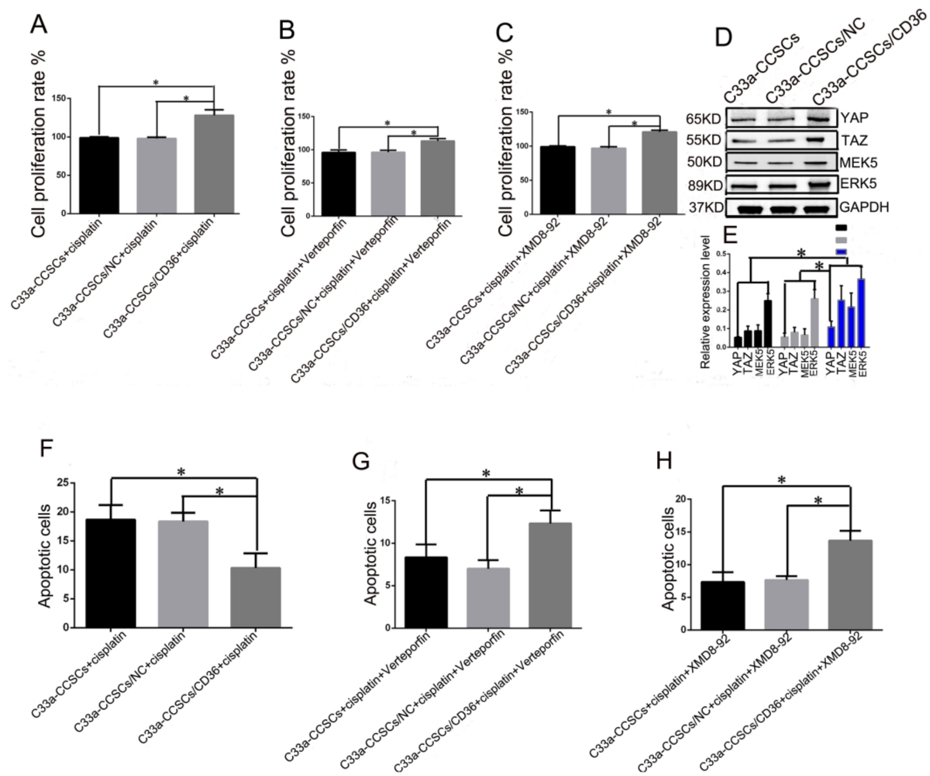

Figure 5. The effects of CD36 expression on chemotherapy resistance of cervical cancer stem cells. A: CD36 promotes proliferative ability of C33a-CCSCs. B,C: Verteporfin and XMD8-92 inhibited proliferation of C33a-CCSCs to some extent. D,E: CD36 increased the the expression levels of YAP, TAZ and ERK5. F: CD36 inhibited apoptosis of C33a-CCSCs. G: Verteporfin promotes apoptosis of C33a-CCSCs. H: XMD8-92 promotes apoptosis of C33a-CCSCs. All experiments were performed in triplicate. *P<0.05.

465x365mm (300 x 300 DPI)

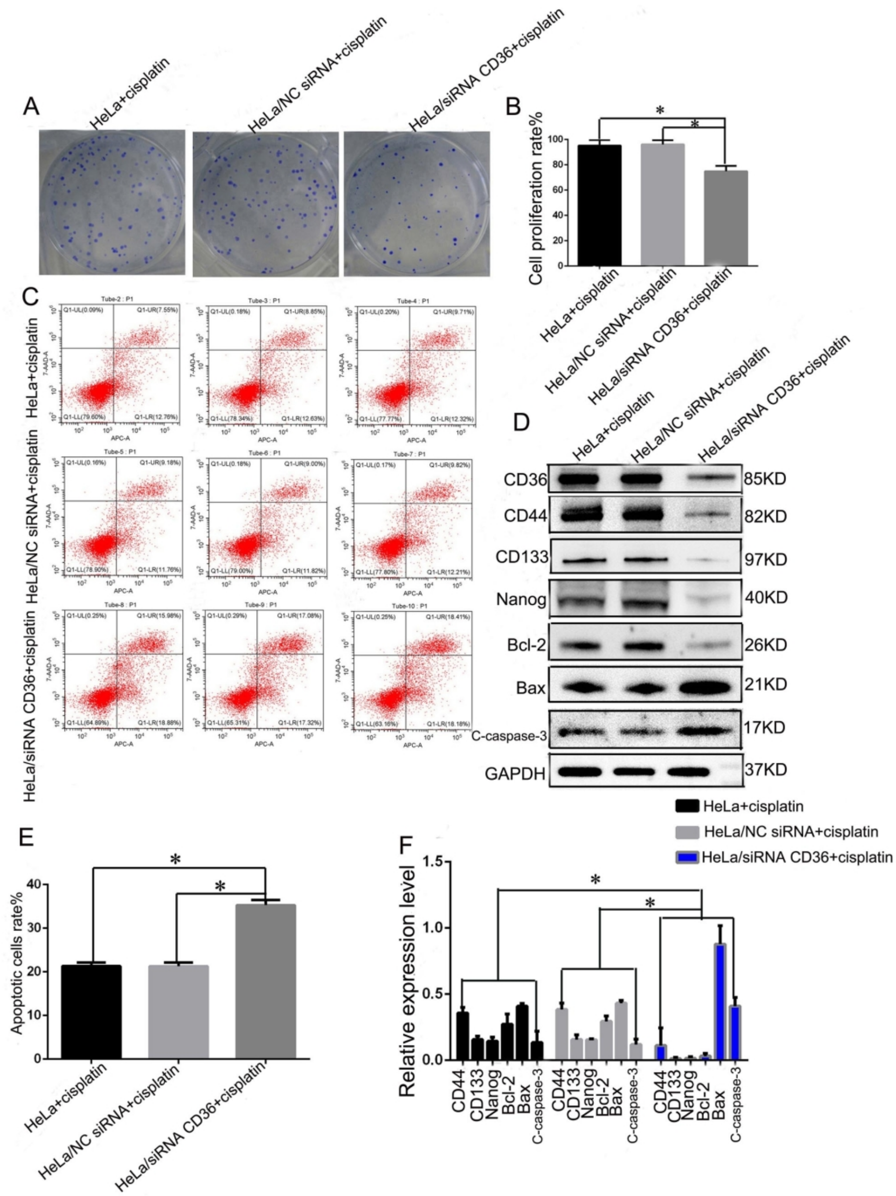

Figure 6. Effects of interfering CD36 expression on chemotherapy resistance of Hela cells. A: Interfering CD36 expression inhibited clone formation ability of HeLa cells after treated with cisplatin. B: Interfering CD36 expression inhibited proliferative ability of HeLa cells after treated with cisplatin. C, E: Interfering CD36 expression promoted apoptosis of HeLa cells after treated with cisplatin. D, F: Compared with the control groups, expression of CD44, CD133, Nanog, Bcl-2 were decreased and expression of Bax, Caspase-3 were increased in the HeLa/siRNA CD36 group. All experiments were performed in triplicate.*P<0.05.

169x221mm (300 x 300 DPI)

gene	time	OS	Stage	CD36	status
TCGA-JX-A3Q0-	212.5	0	Stage III	0.106334	0
TCGA-VS-A9UD-	24.63333	0	Stage IIIA	0.379796	0
TCGA-VS-A950-	40.7	0	Stage IIIA	3.011863	1
TCGA-LP-A5U2-	0.3	0	Stage IIIB	0.072316	0
TCGA-C5-A1BQ-	20.13333	1	Stage IIIB	0.079746	0
TCGA-FU-A40J-	14.2	0	Stage IIIB	0.11357	0
TCGA-DR-A0ZM-	59.7	0	Stage IIIB	0.118669	0
TCGA-DG-A2KJ-	96.43333	0	Stage IIIB	0.154352	0
TCGA-FU-A23K-	12.4	0	Stage IIIB	0.200696	0
TCGA-C5-A7X3-	9.466667	1	Stage IIIB	0.269161	0
TCGA-BI-A0VR-	50.16667	0	Stage IIIB	0.340719	0
TCGA-FU-A770-	1.133333	0	Stage IIIB	0.380776	0
TCGA-EK-A2PI-	19.53333	0	Stage IIIB	0.397804	0
TCGA-C5-A1MN-	41.5	1	Stage IIIB	0.427787	0
TCGA-DG-A2KK-	83.2	0	Stage IIIB	0.457832	0
TCGA-VS-A8EC-	47.16667	0	Stage IIIB	0.490488	0
TCGA-EA-A6QX-	24.33333	0	Stage IIIB	0.498557	0
TCGA-LP-A4AU-	11.43333	0	Stage IIIB	0.530072	0
TCGA-C5-A1BI-	37.06667	0	Stage IIIB	0.55122	0
TCGA-EK-A3GN-	0.9	0	Stage IIIB	0.55288	0
TCGA-VS-A9UL-	14.73333	1	Stage IIIB	0.605414	1
TCGA-MA-AA43-	11.53333	0	Stage IIIB	0.610311	1
TCGA-ZX-AA5X-	3.966667	0	Stage IIIB	0.765881	1
TCGA-C5-A7UH-	132.9333	0	Stage IIIB	0.779847	1
TCGA-EA-A3QD-	13.23333	0	Stage IIIB	0.958895	1
TCGA-C5-A1MH-	39.53333	1	Stage IIIB	1.105976	1
TCGA-EK-A2GZ-	12.76667	0	Stage IIIB	1.20161	1
TCGA-VS-A954-	57.13333	0	Stage IIIB	1.286538	1
TCGA-FU-A3TQ-	26.5	0	Stage IIIB	1.364193	1
TCGA-HM-A4S6-	15.13333	0	Stage IIIB	1.602762	1
TCGA-DS-A3LQ-	23.3	0	Stage IIIB	1.664361	1
TCGA-MA-AA3X-	19.83333	0	Stage IIIB	2.007529	1
TCGA-UC-A7PG-	12.33333	1	Stage IIIB	2.123608	1
TCGA-EA-A44S-	12.3	0	Stage IIIB	2.133504	1
TCGA-C5-A1MK-	2.466667	1	Stage IIIB	2.269569	1
TCGA-FU-A5XV-	10.7	0	Stage IIIB	2.381891	1
TCGA-VS-A8EB-	10.16667	1	Stage IIIB	2.912379	1
TCGA-EK-A2PL-	0.433333	0	Stage IIIB	3.820598	1
TCGA-C5-A2LZ-	101.5333	1	Stage IIIB	4.217823	1
TCGA-C5-A7CL-	15.7	1	Stage IIIB	4.889445	1
TCGA-VS-A8EH-	32.86667	0	Stage IIIB	6.708641	1
TCGA-VS-A953-	15.9	1	Stage IVA	0.070301	0
TCGA-VS-A9V4-	4.4	1	Stage IVA	0.21431	0
TCGA-C5-A7CK-	136.2	1	Stage IVA	0.324765	0
TCGA-VS-A8QC-	11.66667	1	Stage IVA	0.463472	0
TCGA-VS-A9UH-	47.56667	0	Stage IVA	0.726318	1
TCGA-VS-A9UV-	3.466667	1	Stage IVA	0.823503	1
TCGA-DS-A1O9-	8.866667	1	Stage IVA	1.211253	1
TCGA-VS-A8EK-	27.63333	1	Stage IVA	2.647716	1
TCGA-EA-A50E-	7.566667	1	Stage IVA	4.472247	1
TCGA-VS-A9V1-	5.233333	1	Stage IVB	0.076624	0
TCGA-IR-A3LI-	83.1	0	Stage IVB	0.089749	0
TCGA-EX-A449-	14.9	0	Stage IVB	0.100071	0

TCGA-EK-A2RB-	0.3	0	Stage IVB	0.158049	0
TCGA-C5-A7X5-	13.8	1	Stage IVB	0.238642	0
TCGA-VS-A9UY-	18.5	1	Stage IVB	0.332576	0
TCGA-VS-A9UM-	27.63333	1	Stage IVB	0.444087	0
TCGA-VS-A9U6-	44	0	Stage IVB	0.485612	0
TCGA-HM-A6W2-	9.566667	0	Stage IVB	0.935705	1
TCGA-VS-A8QM-	31.7	1	Stage IVB	1.552829	1
TCGA-JW-A5VH-	3.333333	1	Stage IVB	3.769822	1
TCGA-VS-A9V3-	18	0	Stage IVB	6.390622	1

ID	CD36-exp	Axitinib	AZD6482	AZD7762	AZD8055	Bortezomi	Camptothe
TCGA-BI-A0VR-01A	0.340719	3.660418	3.420336	-0.22302	0.347645	-5.39689	-4.39713
TCGA-C5-A1BI-01B	0.55122	3.821308	3.355618	0.432887	0.346588	-5.32694	-3.87563
TCGA-C5-A1BQ-01C	0.079746	3.443232	3.872432	-0.41587	0.344161	-4.75723	-3.96468
TCGA-C5-A1MH-01A	1.105976	3.701603	3.575336	-0.3089	0.310564	-5.74141	-4.30453
TCGA-C5-A1MK-01A	2.269569	3.77154	3.093486	0.474939	0.393432	-4.97088	-3.87943
TCGA-C5-A1MN-01A	0.427787	3.821797	3.650097	0.373932	0.457148	-5.71754	-4.25826
TCGA-C5-A2LZ-01A	4.217823	3.645571	3.404802	-0.15555	0.355855	-5.12616	-4.35561
TCGA-C5-A7CK-01A	0.324765	3.44768	3.814793	0.326722	0.344459	-5.53381	-3.42399
TCGA-C5-A7CL-01A	4.889445	3.4843	3.770544	0.546695	0.400899	-5.17453	-3.63285
TCGA-C5-A7UH-01A	0.779847	3.381721	4.207259	-0.45736	0.333283	-4.56416	-3.25684
TCGA-C5-A7X3-01A	0.269161	3.217006	4.354462	-0.13998	0.328243	-5.4701	-4.61812
TCGA-C5-A7X5-01A	0.238642	3.603288	4.655408	-0.55578	0.403608	-5.17632	-3.38106
TCGA-DG-A2KJ-01A	0.154352	3.515706	5.437954	0.370926	0.414918	-6.45373	-3.70228
TCGA-DG-A2KK-01A	0.457832	3.616131	3.660089	-0.06385	0.375872	-5.66756	-3.5361
TCGA-DR-A0ZM-01A	0.118669	3.196214	3.903703	-0.29216	0.351021	-5.22454	-4.36823
TCGA-DS-A1O9-01A	1.211253	3.575349	3.030317	-0.28671	0.360602	-6.07878	-4.51177
TCGA-DS-A3LQ-01A	1.664361	3.883861	4.59546	-0.10492	0.326878	-5.76496	-3.02048
TCGA-EA-A3QD-01A	0.958895	3.359368	3.995161	0.126281	0.235859	-5.15652	-4.7216
TCGA-EA-A44S-01A	2.133504	3.80991	3.331296	0.261129	0.343101	-5.2033	-3.88294
TCGA-EA-A50E-01A	4.472247	3.431899	3.693166	-0.84592	0.328962	-5.15719	-3.66776
TCGA-EA-A6QX-01A	0.498557	4.077666	3.238327	0.422503	0.396389	-5.97338	-3.9408
TCGA-EK-A2GZ-01A	1.20161	3.789138	3.872351	0.173717	0.423928	-5.25097	-3.90783
TCGA-EK-A2PI-01A	0.397804	3.67011	3.399298	0.32117	0.373241	-4.80234	-3.6763
TCGA-EK-A2PL-01A	3.820598	3.708437	3.627253	0.39672	0.438634	-5.02046	-3.23183
TCGA-EK-A2RB-01A	0.158049	3.863114	3.830147	0.199523	0.417271	-5.37024	-4.24342
TCGA-EK-A3GN-01A	0.55288	3.332777	4.092873	-0.37161	0.373236	-5.50629	-4.44259
TCGA-EX-A449-01A	0.100071	3.572283	3.572704	1.189197	0.39479	-5.17276	-2.88618
TCGA-FU-A23K-01A	0.200696	2.877506	4.767843	-0.07508	0.257939	-5.94106	-5.38521
TCGA-FU-A3TQ-01A	1.364193	3.881185	3.315823	0.36409	0.399608	-5.1765	-3.14189
TCGA-FU-A40J-01A	0.11357	3.4372	3.799475	0.504944	0.366681	-5.87639	-3.95308
TCGA-FU-A5XV-01A	2.381891	3.836095	3.972429	0.64052	0.456533	-5.62644	-3.28136
TCGA-FU-A770-01A	0.380776	3.774985	4.147668	0.011399	0.429967	-5.10582	-3.30846
TCGA-HM-A4S6-01A	1.602762	3.33701	2.95623	-0.29611	0.313672	-5.017	-4.53611
TCGA-HM-A6W2-01A	0.935705	2.074919	3.132999	-0.15226	0.163985	-5.07618	-4.27599
TCGA-IR-A3LI-01A	0.089749	3.947109	4.246733	0.630191	0.492138	-4.76356	-2.73612
TCGA-JW-A5VH-01A	3.769822	2.735463	4.182868	0.267541	0.216361	-4.72408	-4.19689
TCGA-JX-A3Q0-01A	0.106334	3.691324	3.786072	0.027878	0.371796	-6.02767	-4.05645
TCGA-LP-A4AU-01A	0.530072	3.372171	3.818428	0.599816	0.365407	-5.78797	-3.2197
TCGA-LP-A5U2-01A	0.072316	2.711675	5.421288	-0.443	0.196039	-4.92803	-5.47903
TCGA-MA-AA3X-01A	2.007529	3.867088	3.978834	0.28035	0.393076	-4.30736	-2.64029
TCGA-MA-AA43-01A	0.610311	2.947961	3.720534	0.284293	0.308717	-5.86009	-4.22463
TCGA-UC-A7PG-01A	2.123608	3.763666	3.363524	0.824915	0.40612	-4.65957	-2.75298
TCGA-VS-A8EB-01A	2.912379	2.908252	4.236173	-0.71428	0.319418	-5.23914	-4.26459
TCGA-VS-A8EC-01A	0.490488	3.520431	4.173122	0.59125	0.278654	-3.93276	-4.01361
TCGA-VS-A8EH-01A	6.708641	3.712462	4.213105	0.437219	0.415806	-4.76044	-3.47403
TCGA-VS-A8EK-01A	2.647716	3.815696	3.535534	0.072239	0.364936	-4.76463	-3.04937
TCGA-VS-A8QC-01A	0.463472	3.704734	3.435021	-0.09885	0.349535	-5.6289	-3.30529
TCGA-VS-A8QM-01A	1.552829	3.57686	2.879315	0.083879	0.295933	-5.53267	-3.8583
TCGA-VS-A950-01A	3.011863	3.724383	3.889678	-0.29355	0.387764	-4.75334	-3.84142

TCGA-VS-A953-01A	0.070301	3.033737	4.363747	-0.32202	0.29878	-5.0041	-4.87205
TCGA-VS-A954-01A	1.286538	3.111671	3.793244	-0.50902	0.296277	-4.77603	-3.91262
TCGA-VS-A9U6-01A	0.485612	3.302373	3.427697	-0.2741	0.351269	-4.23242	-3.83392
TCGA-VS-A9UD-01A	0.379796	3.408373	4.742586	0.038005	0.303645	-5.46668	-4.63593
TCGA-VS-A9UH-01A	0.726318	3.247305	3.966814	-1.06353	0.319375	-6.26988	-5.07129
TCGA-VS-A9UL-01A	0.605414	3.102712	3.57481	1.033875	0.310092	-3.09785	-3.89715
TCGA-VS-A9UM-01A	0.444087	3.415696	2.453643	0.241226	0.332617	-5.14557	-3.61167
TCGA-VS-A9UV-01A	0.823503	3.643072	3.569784	0.104707	0.348375	-5.65504	-4.08504
TCGA-VS-A9UY-01A	0.332576	3.527999	3.017786	-0.05229	0.362303	-5.73103	-4.35238
TCGA-VS-A9V1-01A	0.076624	3.532575	3.893978	1.00086	0.435788	-4.90999	-3.19394
TCGA-VS-A9V3-01A	6.390622	3.598269	3.134113	0.524616	0.390481	-5.17532	-4.0378
TCGA-VS-A9V4-01A	0.21431	3.448576	5.621583	1.48837	0.488987	-4.78114	-2.76515
TCGA-ZX-AA5X-01A	0.765881	3.386493	3.412547	-0.73809	0.321007	-5.26508	-3.95934

Cisplatir	Dasatinik	Erlotinik	Gefitinik	Gemcitabi	GSK269962	Lapatinik	Nilotinik	Paclitaxe
0.950916	2.16146	4.292524	1.942194	-2.68046	3.885778	4.496173	4.073465	-3.3324
1.280191	2.040422	4.09688	1.46317	-2.33814	3.720014	4.127864	4.074138	-3.22221
0.791731	2.270998	4.281362	1.04146	-2.45544	4.086031	4.438828	3.936381	-2.03606
0.862976	1.588231	4.478878	1.840501	-2.73868	3.585858	4.423051	3.797859	-3.46813
1.347367	1.684216	4.602803	1.706186	-2.26619	3.537105	4.282921	4.20859	-2.46862
0.517843	-0.44383	3.942941	1.676915	-2.60342	3.310771	3.595736	4.543347	-3.28083
0.644857	2.195087	4.048214	1.507163	-2.53056	4.183922	4.100727	3.757197	-3.39065
1.107352	1.72778	4.242914	2.203004	-2.40587	3.4335	4.539429	4.363176	-2.96877
1.269807	2.211728	4.331621	1.797745	-2.12939	4.103936	4.718706	4.143335	-1.99005
0.815662	2.4743	4.41821	1.341986	-2.40724	3.422286	4.587734	3.99647	-3.19434
0.20158	1.608899	4.154716	1.971757	-2.79699	3.2249	4.440855	4.511948	-2.94607
0.435063	1.592724	4.263558	2.304	-2.69002	3.683328	4.039312	4.201815	-2.883
0.949452	0.684987	4.058886	0.919584	-1.60783	3.292487	3.980774	4.395927	-3.83971
0.824511	2.460132	4.442929	2.165901	-2.2297	3.382978	4.449434	4.214166	-2.64095
0.614431	0.809084	3.809476	0.500197	-2.30752	3.73032	3.849072	3.847458	-3.15874
0.875313	0.129579	4.284747	1.759617	-2.55637	3.265818	4.111758	4.078554	-3.01377
1.218169	1.442366	3.79738	2.329499	-2.24124	3.75342	3.899908	4.346014	-2.5397
1.328728	3.381758	4.43067	1.235639	-2.7553	3.806557	5.048806	3.875422	-2.56183
1.454748	3.06338	4.200706	1.115945	-2.33515	4.100987	4.15903	4.158105	-2.82483
0.551063	1.544337	4.34692	1.443783	-2.58665	3.61115	4.232647	4.176752	-2.75066
1.502916	1.866474	3.460722	1.347625	-2.41153	4.012389	3.771293	4.064609	-3.28292
0.571408	1.701636	4.204792	1.973101	-2.32644	3.924281	3.778543	4.52083	-2.55107
1.177973	2.133603	3.638119	1.773845	-2.18676	3.594448	3.949456	4.342443	-2.3834
1.488192	0.852337	3.885256	1.006714	-2.25582	3.574798	3.353923	4.271532	-3.58069
0.813896	2.462181	3.767896	1.161985	-2.26427	3.65704	3.428604	4.422827	-3.98214
-0.46544	2.107433	3.975548	2.190334	-2.61331	3.551901	4.329774	4.275381	-3.41578
1.812286	4.136732	4.832369	3.726508	-1.89225	3.873202	4.416812	4.587459	-2.67936
0.264727	1.954422	4.766934	1.930096	-2.51423	2.901969	4.994495	4.40953	-3.79134
1.197446	1.781702	4.609894	1.793427	-2.26321	3.759707	4.228811	4.048684	-3.13732
0.613462	1.977146	3.949335	1.813302	-2.57108	3.545913	4.438464	3.832837	-2.89604
1.322097	0.603233	3.451542	1.263522	-2.32832	4.08119	3.459017	4.226727	-4.0684
0.704233	1.761162	4.563335	2.060188	-2.31911	4.081772	4.226451	4.172772	-2.67134
0.530375	1.923662	4.438524	1.672812	-2.56336	3.848121	4.389686	3.712072	-2.74779
0.66104	2.862238	4.773831	3.392513	-2.56757	3.471464	4.802865	4.38787	-1.37242
1.247729	2.335702	4.536737	2.339807	-1.47514	4.032506	4.017111	4.704782	-2.70531
0.370405	4.412203	5.185329	3.586953	-2.63729	3.121692	5.359177	4.545868	-1.76626
0.598716	1.421097	4.141602	2.088766	-2.54957	3.869666	4.193122	3.9488	-3.42172
0.778483	1.79602	4.293053	2.179184	-2.30627	3.566302	4.259526	4.494897	-3.02637
-0.29877	3.601592	4.4615	1.88245	-3.27667	3.533725	5.076574	3.68089	-2.74268
1.830428	2.229908	5.007963	2.076224	-2.07038	4.420872	4.686158	4.20891	-2.55894
0.237193	-0.39311	4.556381	3.017218	-2.50775	2.196241	4.678821	4.364137	-3.21134
1.746707	1.921272	4.382228	1.85471	-1.9947	3.842081	4.273502	4.289822	-2.42524
0.178984	1.256453	4.013303	1.974692	-2.67835	2.801132	4.170863	4.327984	-3.35409
1.131657	3.732407	4.142123	2.221708	-2.38159	4.103348	4.55681	4.428819	-2.5883
0.669996	2.040609	3.5454	1.842844	-2.26414	4.022135	3.584562	4.254799	-3.27743
1.117571	2.837008	4.237654	1.679256	-2.52172	4.172164	4.240442	3.935036	-2.41273
0.926228	1.73848	3.980862	1.799391	-2.31361	3.102586	4.076423	4.223387	-3.30432
1.035877	1.373136	4.057072	1.67835	-2.48503	3.539969	4.274614	3.801111	-3.27714
0.552994	2.46457	4.520832	2.141806	-2.38556	3.623907	4.49742	4.645754	-2.73316

−0.23502	1.788667	4.740385	1.392294	−2.84267	3.260118	5.038803	4.227554	−3.24122
0.614678	2.13734	4.703801	1.589829	−2.39352	3.535996	4.706318	4.158191	−3.12304
0.28043	2.452917	4.56252	2.197038	−2.36584	3.91761	4.70694	3.900582	−1.91587
1.130884	3.009235	4.458021	2.084026	−2.51809	3.543144	4.897084	4.402465	−3.46615
0.275101	0.916707	4.339056	1.502846	−2.80574	2.948225	4.705291	4.09066	−3.22035
1.418336	4.883698	5.457504	3.401156	−2.01118	3.991336	5.481452	4.164013	−1.13256
1.60786	1.750575	4.259087	1.926549	−2.25013	3.799057	4.242302	3.73774	−2.83269
0.737659	2.777494	4.382401	1.905761	−2.42909	3.794484	4.324793	4.28861	−2.93146
0.729908	1.123077	4.169695	1.577653	−2.73642	4.112842	4.351852	3.847051	−3.15063
0.817987	3.628466	4.91696	2.830861	−1.95184	3.979	4.599951	4.616956	−1.98749
1.504162	2.55454	4.162554	1.735807	−2.32825	4.128369	4.41867	4.004019	−2.45378
0.399013	4.452284	4.873152	2.939835	−2.14496	4.620983	4.985564	4.367707	0.220104
0.553907	0.800853	4.237066	1.872171	−2.59983	3.265563	4.524342	3.763652	−2.64762

Rapamycir	Sorafenit	Vinblasti	Vinorelbi	Vorinostat
-0.36763	3.926204	-4.40076	-4.05869	1.217697
-0.31151	3.888592	-3.63604	-3.58695	1.165243
0.128674	3.837066	-4.32029	-3.08184	1.452139
-0.50805	3.749559	-4.58345	-4.02613	1.073707
0.279735	3.978286	-4.12423	-3.89331	1.174451
0.368181	3.85032	-4.04935	-3.41349	1.529692
-0.3731	3.828889	-4.17399	-4.25532	1.042122
0.105372	3.924886	-3.96709	-3.79634	1.467364
0.334165	3.899985	-3.89481	-3.31695	1.725247
-0.43777	3.678772	-3.86615	-3.29145	1.100983
-0.46275	3.790866	-4.86329	-3.48791	0.954243
0.553332	3.738785	-3.76892	-3.27325	1.633627
-1.27594	3.6282	-4.32662	-0.11353	1.68845
-0.32188	3.999454	-3.55938	-3.12191	1.268514
0.378836	3.885065	-4.70798	-3.25526	1.1478
-0.33231	3.875805	-4.8022	-3.57573	1.452164
0.15774	3.878174	-3.64028	-3.13453	1.505887
-0.2942	3.799399	-4.58929	-3.31525	0.736583
-0.16274	3.938977	-4.02878	-3.50966	1.144405
0.339959	3.696684	-4.29893	-3.64355	1.129735
-0.98141	3.797168	-3.77963	-3.51738	1.445567
0.319482	3.764885	-3.75126	-3.44114	1.821458
-0.23965	4.004999	-2.82277	-3.71277	1.878713
-0.5309	3.863681	-4.05085	-4.03054	1.578255
-0.6203	3.784875	-4.71775	-3.81338	1.548686
0.132469	3.827771	-4.33933	-3.93456	1.159707
-1.97817	3.819072	-3.16193	-2.76322	1.905009
-1.06849	3.743708	-5.44707	-2.51057	0.634287
-0.1235	3.990329	-4.58515	-4.47038	1.419217
-0.55713	3.969997	-2.65633	-3.06668	1.197902
0.174358	3.723432	-4.02699	-4.11465	1.427325
-0.18149	4.001736	-2.93104	-3.07576	1.524144
-0.06503	3.85991	-4.71869	-4.15232	1.107298
-0.35691	3.831306	-4.22983	-3.91501	0.666758
-0.47534	4.011108	-2.87439	-2.42466	1.981495
-0.44922	3.814991	-3.93583	-4.15772	0.654949
-0.61335	3.895003	-4.544	-3.91173	1.394981
-0.06237	3.786951	-3.82227	-3.82406	1.270271
0.58384	3.634564	-5.36115	-3.64019	0.004422
0.127203	3.929562	-3.36072	-3.36411	1.447872
0.089595	3.976097	-4.34157	-3.36803	1.00532
0.300597	4.023689	-3.40491	-3.59374	1.419987
-0.56261	3.655679	-3.74696	-3.45268	1.16362
-0.74413	3.911855	-3.61467	-3.94177	1.052804
0.153929	3.75463	-4.01052	-4.39556	1.880747
0.187387	3.918333	-3.55395	-4.14387	1.264746
-0.4069	3.816594	-4.18094	-3.75712	1.159898
-0.43469	3.907158	-4.0395	-3.99742	1.078783
-0.32198	3.782265	-3.9522	-3.4632	1.521566

-0.00975	3.917778	-4.33664	-3.35705	0.857542
0.129326	3.908113	-4.46493	-3.97244	0.817574
-0.01661	3.791662	-3.73169	-3.84264	1.304176
-1.51812	3.673048	-5.13845	-3.24524	1.347883
-0.39385	3.757053	-5.18885	-3.02747	1.19654
-0.14838	4.185658	-3.66177	-3.42134	1.277418
-0.13575	3.838325	-4.19894	-4.02974	1.055105
-0.13564	3.727249	-3.96745	-3.93668	1.185539
0.064978	3.933326	-4.02753	-4.11291	1.073728
-0.60133	3.816778	-2.84908	-2.57004	1.644087
-0.27338	4.045093	-3.41993	-3.16614	1.345514
0.962058	3.821037	-0.93194	-1.41253	0.937295
0.180313	3.904889	-4.17795	-3.72743	0.915782

ID	p	Cor
FABP4	4.16E-07	0.591409
NRG4	5.83E-07	0.585338
SPINK9	7.28E-06	0.535555
CLN8	1.38E-05	0.521561
ARL5A	1.61E-05	0.518079
ARRDC4	3.99E-05	0.496895
CARTPT	4.22E-05	0.495513
LCE4A	4.97E-05	0.49155
SLC13A5	5.31E-05	0.489925
FABP9	5.98E-05	0.486948
LYSMD4	7.42E-05	0.481545
OR13A1	8.42E-05	0.478334
SRRM3	0.00011	0.471306
CHMP4C	0.000114	0.47045
YAP	0.000119	0.469322
KRTAP4.4	0.000122	0.468766
GCNT4	0.000126	0.467782
C4orf17	0.000147	0.463735
KRT10	0.000148	0.463557
TMEM79	0.000152	0.462754
GNAI1	0.000163	0.460891
GAN	0.000166	0.460428
C22orf23	0.000169	0.45993
ACKR3	0.000176	0.458944
ZMIZ1	0.000178	0.458537
MEK5	0.000189	0.457009
CHRNA3	0.000195	0.456124
TMEM45A	0.000221	0.452625
EPHA4	0.000224	0.452266
RAB10	0.000227	0.45184
USH1G	0.000251	0.449117
SLC12A6	0.000257	0.448422
PGLYRP4	0.000262	0.447904
TAZ	0.000266	0.447494
REL	0.000274	0.446642
DUSP13	0.000279	0.446069
MDM2	0.00028	0.446018
FZD10	0.000313	0.442806
PSAPL1	0.000325	0.441764
BNIPL	0.000338	0.440647
LENEP	0.000338	0.440615
CD44	0.000342	0.440306
ACVR1C	0.000348	0.439765
RORA	0.000361	0.438756
ERK5	0.000362	0.438632
SEMA3C	0.000399	0.435854
KCNK7	0.000403	0.435577
TMEM155	0.000407	0.435224
CST8	0.000408	0.435179
STAU2	0.000412	0.43489
SPTBN5	0.000416	0.434645
ATAD2B	0.000424	0.43409
FBXO22	0.000425	0.434004

TNFRSF10I	0.000427	0.43388
CD133	0.000429	0.43375
TGM5	0.000433	0.433455
PIGF	0.000443	0.43278
PGLYRP3	0.000446	0.432596
RAB18	0.000448	0.432424
KLHL20	0.000456	0.43189
CEL	0.000469	0.431108
NTRK3	0.000481	0.430357
TMEM68	0.000489	0.429835
C1orf61	0.000491	0.429738
HIST2H2BI	0.000532	0.427353
SPANXN1	0.000547	0.426483
LRRK1	0.000557	0.425972
TMEM184A	0.000558	0.42591
TMEM254	0.000561	0.425718
PAQR7	0.000605	0.423446
VPS37A	0.000607	0.423343
IPMK	0.000616	0.422926
LIPK	0.000627	0.422353
PRSS42	0.000652	0.421195
LYPD3	0.000676	0.420087
UNC5B	0.000728	0.417797
FAM84A	0.000734	0.417543
CPNE3	0.000754	0.41674
GPR1	0.000768	0.416142
TPST2	0.000773	0.415939
DLX5	0.000778	0.415738
ARL8B	0.000803	0.414769
RALGPS2	0.000814	0.414358
RIC3	0.000844	0.413208
RALGAPA1	0.000854	0.41284
CHP2	0.000856	0.412777
SCN3A	0.000869	0.412291
SLC6A14	0.000878	0.411964
CHRNB4	0.000881	0.411851
YPEL5	0.000912	0.410769
SECISBP2I	0.000927	0.410267
BICD2	0.000928	0.410246
RXRA	0.000936	0.409972
BAALC	0.00096	0.409149
PIGN	0.000968	0.408891
CYP4F3	0.000968	0.408882
NCKAP1	0.000992	0.40813
ERMP1	0.000994	0.408051
FBXW2	0.001006	0.407686
SNX16	0.001013	0.407441
SKIL	0.001024	0.407109
ZMAT3	0.001032	0.406859
TMEM117	0.001039	0.406651
PGM2	0.001081	0.405368
CST9L	0.001099	0.404845
ANKRD2	0.001105	0.404674
ADAD2	0.001112	0.404478

FZD6	0.001125	0.404105
GRHL1	0.001136	0.403782
RIMS3	0.001155	0.403251
LCE2D	0.001203	0.40194
NOTCH3	0.001213	0.40167
INTU	0.001221	0.401441
AADAC	0.001224	0.401362
MYO1H	0.001226	0.401316
SH3GLB2	0.001232	0.401153
KLHL28	0.001233	0.401147
CLIP1	0.001252	0.400643
SERPINB3	0.00127	0.400182
FAM219B	0.001297	0.399482
MXD1	0.0013	0.39942
LRRC57	0.001323	0.398833
SLC6A11	0.001328	0.398711
KLHL42	0.001335	0.398555
MPP7	0.001339	0.398454
RC3H1	0.001361	0.397906
NEMF	0.001378	0.397511
TBC1D2B	0.00141	0.396756
ABCA5	0.001446	0.395925
ALAD	0.001446	0.395925
BTG1	0.001463	0.395529
HOXD4	0.00147	0.395387
FRRS1	0.001471	0.395361
AMFR	0.001484	0.395063
TANC1	0.001488	0.394987
FLG2	0.00152	0.394272
LCE2C	0.001536	0.393931
SLC4A9	0.001556	0.39349
DCST1	0.001565	0.393308
ABI1	0.00159	0.392784
AGL	0.001614	0.392278
SLC37A2	0.001619	0.392171
KIFAP3	0.001638	0.391779
CCR3	0.00165	0.391545
TXNDC8	0.001664	0.391261
DSG4	0.001664	0.39126
IVNS1ABP	0.001672	0.391089
FAM206A	0.001672	0.391089
CNDP1	0.001687	0.390789
GNAL	0.00173	0.389951
TP53INP1	0.00174	0.389753
IPPK	0.001742	0.389722
NR6A1	0.001742	0.389719
SYCN	0.00175	0.389571
CALCRL	0.001754	0.389487
PUS10	0.001764	0.389304
KIAA1841	0.001768	0.389218
CDK5R1	0.001799	0.38864
CREG1	0.001803	0.388555
GPR155	0.001811	0.388416
ESRP2	0.001824	0.38817

CHST2	0.001825	0.388147
C18orf25	0.001836	0.387943
STEAP4	0.001857	0.387557
USP8	0.001858	0.387538
MAST4	0.001862	0.387477
LCE3E	0.001896	0.386867
RNF111	0.001949	0.385918
LRRC28	0.001998	0.385072
PHLDB3	0.002018	0.384739
FAM214A	0.00203	0.384534
AKTIP	0.002032	0.384502
HS6ST3	0.002048	0.384232
FAM214B	0.00205	0.384194
NPL	0.002053	0.384158
MAP2K1	0.002098	0.383416
ZNF106	0.002106	0.383278
RHCG	0.002121	0.383039
DNAJB4	0.002125	0.382974
DPP8	0.002128	0.382922
ABHD2	0.002154	0.382499
UBE2V2	0.00218	0.382088
CMIP	0.002186	0.381996
HDAC4	0.002196	0.381835
ATP9B	0.002202	0.381738
RNF217	0.002206	0.38169
PTPDC1	0.002217	0.38151
BNIP2	0.002243	0.381104
ATP6V1A	0.002277	0.380595
KCTD11	0.002281	0.380522
LPCAT3	0.002291	0.380378
PRKACB	0.002341	0.379631
YTHDF3	0.002348	0.379526
ZNF770	0.002392	0.378877
ZBTB1	0.002406	0.378674
RALGDS	0.002429	0.378343
SYPL1	0.002434	0.378279
MALT1	0.002447	0.378087
CCDC144A	0.002478	0.377646
ATG14	0.002519	0.37707
EPHB3	0.002547	0.376696
HOXD1	0.002568	0.376402
C9orf85	0.00258	0.376238
CELA2B	0.002598	0.376001
SLC23A2	0.002624	0.375645
MAP3K2	0.002649	0.37531
NAB1	0.002661	0.375158
PTBP3	0.002704	0.374593
CAPNS2	0.002713	0.374471
SAMD8	0.002759	0.373885
WWP1	0.002767	0.37377
ARIH1	0.002796	0.373412
OR1Q1	0.0028	0.373353
COBLL1	0.002827	0.37302
NIPAL2	0.002843	0.372819

KRTAP5.11	0.002875	0.372422
HYAL1	0.002892	0.372217
ZNF117	0.002935	0.371685
RAB14	0.002947	0.371539
ABCA1	0.003002	0.370883
C15orf41	0.003047	0.370357
STXBP5	0.003073	0.370051
MOB4	0.003099	0.369743
EVPL	0.003107	0.36966
CA6	0.003128	0.36941
RASAL2	0.00317	0.368936
NANOS1	0.003178	0.368847
AXDND1	0.003213	0.368451
PTGS1	0.003232	0.368246
ARL15	0.00327	0.367822
RNASE10	0.003302	0.367476
ZNF236	0.003303	0.367458
PCMTD1	0.003326	0.367212
HBP1	0.00333	0.367167
SLC22A25	0.003338	0.367083
ART1	0.003343	0.367021
BLOC1S2	0.003385	0.36657
HOOK3	0.003453	0.365861
LRRC8A	0.00352	0.365162
UNKL	0.003534	0.365013
RBP3	0.003597	0.364372
CLU	0.00364	0.363942
KLHL36	0.003642	0.363918
ZNF780A	0.003652	0.363821
COL24A1	0.003688	0.363465
SYK	0.003724	0.363113
ZBTB6	0.003761	0.362747
OR1L3	0.00377	0.36266
TMEM87A	0.003812	0.362252
DAAM1	0.003817	0.362204
MEGF9	0.00386	0.361796
SCAPER	0.003889	0.361517
IMPA1	0.003913	0.361291
PPP1R13L	0.003995	0.360534
PAPOLG	0.004085	0.359708
TSC1	0.00409	0.359665
SLTM	0.004146	0.359165
RETSAT	0.004183	0.358835
KCTD21	0.004184	0.35883
PPP2R2A	0.004192	0.358755
CES4A	0.004235	0.358373
BBS10	0.004236	0.358368
TOM1L2	0.004242	0.358319
ZNF658	0.004262	0.358143
HOXD8	0.004265	0.358119
FAM160B2	0.004273	0.358043
SNTB2	0.004301	0.357802
SLC35G1	0.004502	0.356101
SERPINB7	0.00451	0.356041

PAWR	0.00454	0.355793
P2RY1	0.00455	0.355706
CACNA2D1	0.004561	0.355614
MEX3B	0.004564	0.355592
LONP2	0.004575	0.355501
NGRN	0.00458	0.355463
ZNF385A	0.004617	0.355159
ERICH1	0.004619	0.355148
UBQLN1	0.004684	0.354623
CDC42SE1	0.004789	0.353788
SLC39A2	0.004799	0.353714
PYGL	0.004824	0.353512
MUCL1	0.004933	0.352674
IGIP	0.004946	0.352573
HSPA4L	0.004968	0.352404
PDE2A	0.004979	0.352322
PEX13	0.005014	0.352055
YTHDC2	0.005017	0.352037
XKRX	0.005019	0.35202
RIOK3	0.005038	0.351876
NT5C1B	0.005211	0.350598
HECTD2	0.005217	0.350557
GANC	0.005231	0.350449
ANKRD9	0.005244	0.35036
SP6	0.00525	0.350312
ADAM23	0.005252	0.3503
DSP	0.005291	0.350016
PITPNM2	0.005303	0.34993
GOLGA1	0.005349	0.349603
NOD2	0.005368	0.349471
CNOT7	0.005387	0.349336
ZNF280D	0.005427	0.349049
CEACAM19	0.00544	0.348957
MTA3	0.005458	0.348832
PSMD5	0.005468	0.348766
MTSS1L	0.005543	0.34824
LY6G6C	0.005563	0.348105
OSTF1	0.005585	0.347951
REEP4	0.005636	0.347602
CTSB	0.005652	0.347499
MTMR3	0.005661	0.347433
MBLAC2	0.005705	0.34714
NPC1	0.005751	0.346829
DENND1B	0.005791	0.346564
KRAS	0.005847	0.346196
ESRP1	0.005939	0.345591
EPG5	0.005954	0.345493
RBM11	0.00596	0.345458
PLD1	0.005966	0.345414
PON2	0.005976	0.345349
GAPVD1	0.005985	0.345295
CCL26	0.005999	0.345201
NIPA1	0.006063	0.34479
UACA	0.006106	0.344519

GM2A	0.006138	0.34432
RIT1	0.006173	0.344095
ATP6V1G1	0.006221	0.343799
PTPN12	0.006232	0.343729
MFAP1	0.006233	0.343722
CYB561D1	0.006238	0.343688
ASB7	0.006269	0.3435
CEP350	0.006282	0.343416
SPINK5	0.006293	0.343351
KIFC2	0.00632	0.343185
ERV3.1	0.006358	0.342952
ASPH	0.006361	0.342933
ZNF655	0.006408	0.342645
TMEM40	0.006467	0.342289
TAS2R20	0.006518	0.341981
EPN2	0.006521	0.341962
CHMP1B	0.006538	0.341861
NRBP1	0.006589	0.341556
PCSK5	0.006592	0.341541
SCD	0.006626	0.341338
DUOXA1	0.006669	0.341089
F11R	0.006689	0.340967
ZSCAN29	0.006733	0.340711
CD46	0.006765	0.340528
TMOD3	0.006771	0.34049
TPPP	0.006772	0.340485
ANKRD46	0.006788	0.340395
ABHD17B	0.006788	0.340394
TM7SF3	0.006799	0.340329
TAF7	0.006856	0.340003
CYP3A7	0.006885	0.339835
LCE1D	0.006906	0.339717
PDILT	0.006948	0.339477
SNX33	0.006954	0.339447
ZNF264	0.007032	0.339006
BRMS1L	0.007033	0.338999
CDK17	0.00706	0.338846
ASPA	0.007131	0.338455
SF3B1	0.007145	0.338378
CLIP4	0.007148	0.338361
OSBP2	0.007165	0.338266
FBXO34	0.007225	0.337937
GSN	0.007264	0.337725
PRPF39	0.007386	0.337066
NOTCH1	0.007397	0.337003
CDK8	0.007399	0.336997
LRFN2	0.007422	0.336872
PLEKHA1	0.007438	0.336785
CD58	0.00747	0.336615
CDK9	0.007505	0.336428
ARRDC3	0.007518	0.33636
PCMTD2	0.007519	0.336355
FEM1B	0.007522	0.336341
TMPRSS11I	0.007567	0.336103

NPHP3	0.007589	0.33599
INPP4A	0.00761	0.335877
HSPA2	0.007652	0.335658
NOX5	0.007663	0.335601
WNT11	0.007712	0.335349
MAP7	0.007778	0.335006
RYR1	0.007819	0.334798
ADCY7	0.007824	0.334773
SLURP1	0.007843	0.334675
SOX7	0.007871	0.334533
ATP6V1H	0.007912	0.334326
FUT11	0.007958	0.334095
MIB1	0.00797	0.334035
CST6	0.008026	0.333751
KRT74	0.008081	0.333479
DHX32	0.008098	0.333397
SFT2D2	0.008215	0.33282
NAPG	0.008222	0.332784
GDPGP1	0.008226	0.332767
RAET1G	0.008237	0.33271
GPR157	0.008325	0.332286
LOR	0.008349	0.332171
ACVR1	0.00844	0.331734
ALDH1A3	0.008453	0.331668
RCOR1	0.008479	0.331547
CMTR2	0.008496	0.331466
DSTYK	0.008511	0.331395
BLOC1S6	0.008547	0.331222
ALDH3B2	0.008616	0.330899
HIST1H2BC	0.008622	0.330869
STX17	0.008648	0.33075
WDR37	0.008672	0.330637
SERPINB4	0.008679	0.330602
DHCR24	0.008698	0.330513
RGSL1	0.00878	0.330134
SPINK6	0.008793	0.330074
UNC119B	0.0088	0.330044
TLK1	0.008804	0.330023
GJB6	0.008841	0.329856
TNK2	0.008846	0.329834
WEE2	0.008855	0.32979
NEBL	0.00888	0.329678
NCCRP1	0.008896	0.329602
CHD9	0.008904	0.329566
CDX4	0.008931	0.329443
SLC35G3	0.008974	0.32925
BTBD11	0.009107	0.328649
ARNT	0.009149	0.328462
RAB3GAP2	0.009155	0.328436
PTHLH	0.009178	0.328333
ZNF624	0.0092	0.328238
GALR2	0.009296	0.327811
CLPX	0.0093	0.327794
PPP3R1	0.00932	0.327706

LEPROT	0.009326	0.327679
RBL2	0.009338	0.32763
ABO	0.00936	0.327531
EEA1	0.009381	0.327442
MAPKAP1	0.009418	0.32728
ADAMTS17	0.00943	0.327228
FAM129B	0.009436	0.327202
CDKN2B	0.009455	0.32712
CCDC105	0.009479	0.327016
ATP11B	0.009506	0.326901
PUM2	0.009566	0.326641
TGFA	0.009588	0.326549
OR10A3	0.009747	0.325873
FASTKD1	0.009859	0.325404
LACC1	0.009897	0.325246
DCST2	0.009922	0.325139
DYNC1LI2	0.009926	0.325123
DNAJA4	0.009971	0.32494
CASP14	0.009972	0.324935
VPS13A	0.009996	0.324835
RBBP6	0.010109	0.324371
MME	0.010155	0.324182
GALNT1	0.010172	0.324114
TRAPPC8	0.010202	0.323995
BCL2L2	0.010215	0.323942
CHAC2	0.010258	0.323766
LNX2	0.010307	0.323571
FAM43A	0.010367	0.32333
BTAF1	0.010401	0.323194
KATNBL1	0.010483	0.322868
EFCAB14	0.010484	0.322865
SERPINB8	0.010497	0.322812
SLC35D1	0.010544	0.322628
TMEM132B	0.010553	0.32259
PHF2	0.010563	0.322551
BRWD1	0.010586	0.322462
CNEP1R1	0.010683	0.322083
MORC3	0.0107	0.322019
DMTF1	0.010705	0.321996
PRR23B	0.010714	0.321963
KRTAP19.3	0.010806	0.321609
HDHD2	0.010812	0.321585
WNT5A	0.010827	0.321527
NCOA4	0.010908	0.321217
PRRC2C	0.01093	0.32113
LGALSL	0.010935	0.321112
MFSD6	0.011008	0.320834
ALOXE3	0.011038	0.320722
MTSS1	0.011048	0.320682
TMEM245	0.011057	0.32065
CPEB4	0.011066	0.320616
SCRN3	0.011156	0.320275
MAP4K5	0.011159	0.320267
GFOD1	0.011166	0.320241

ETV3	0.011171	0.320222
UNC45A	0.011287	0.319787
NIN	0.011332	0.31962
NDEL1	0.011378	0.319452
MAP3K9	0.011398	0.31938
SLC44A1	0.011398	0.319379
ADSSL1	0.0114	0.319372
AP4E1	0.011524	0.318917
PPP1R1C	0.011538	0.318866
RRM2B	0.011562	0.318779
IL20RA	0.011572	0.318741
ARAP2	0.011595	0.318659
GDAP2	0.011606	0.318617
PAFAH1B1	0.011621	0.318566
ZBTB37	0.011629	0.318535
PPP2CB	0.011658	0.31843
C9orf3	0.011749	0.318104
MREG	0.011786	0.31797
PLXNB3	0.011833	0.317802
CYFIP1	0.011955	0.317371
SVIL	0.011988	0.317254
MEF2A	0.012023	0.317132
METTL9	0.012044	0.317056
RNF20	0.012076	0.316946
PRDM1	0.012101	0.316859
FAM110A	0.012135	0.316738
ANKRD29	0.012147	0.316699
MYH14	0.01218	0.316584
BCL2L10	0.012192	0.316542
GOLGA2	0.012227	0.316419
SPPL2A	0.012284	0.316224
NMB	0.012303	0.316158
ECM1	0.012311	0.316129
FKTN	0.012329	0.316068
MYO1B	0.012344	0.316016
GALR3	0.012356	0.315976
SOST	0.012412	0.315784
WDR59	0.012494	0.315504
IGFL3	0.012526	0.315396
DMTN	0.012622	0.315069
SOS1	0.01263	0.315045
CTRC	0.012707	0.314786
PIM1	0.012769	0.314578
BARX1	0.01278	0.314541
SPTBN2	0.012893	0.314165
ARHGEF4	0.012997	0.313821
ABHD4	0.013057	0.313627
AANAT	0.013061	0.313612
ANKRD26	0.01313	0.313388
EMP2	0.013135	0.313373
SRPK2	0.013169	0.31326
LIPI	0.013173	0.313247
ITGAV	0.013184	0.313212
PXT1	0.013265	0.31295

RDH16	0.013281	0.312897
TVP23B	0.013303	0.312827
GSDMC	0.013332	0.312733
RAPGEFL1	0.013335	0.312725
SCYL3	0.013347	0.312685
LPAR5	0.013392	0.312542
DUSP11	0.013462	0.312318
ARID4A	0.013464	0.312312
CDC42BPG	0.013526	0.312116
ZNF532	0.013604	0.311868
BMP7	0.013661	0.311687
SBNO1	0.013739	0.311444
SDHC	0.013743	0.311431
CLCA2	0.01378	0.311316
TTC21B	0.013799	0.311256
THEM5	0.013803	0.311242
CHD7	0.013811	0.311217
AADACL2	0.013813	0.311212
SOCS4	0.013832	0.311151
CADM4	0.013859	0.31107
TREML4	0.013877	0.311013
KLC3	0.013906	0.310921
GABRE	0.013919	0.310881
DUOX1	0.013949	0.31079
HAUS2	0.013963	0.310745
UBE2G1	0.013972	0.310719
STAM	0.01406	0.310447
UBE2D1	0.014152	0.310167
STRN	0.014195	0.310033
NCOA3	0.014205	0.310003
RTF1	0.014219	0.309962
SREBF1	0.014265	0.309822
MPP5	0.014391	0.309441
HOXC13	0.014467	0.309212
NACC2	0.014477	0.309185
SCRIB	0.014518	0.30906
RASGRP1	0.014539	0.308997
BAZ2B	0.014548	0.30897
NDST1	0.014575	0.30889
ZKSCAN1	0.014622	0.308752
BEST2	0.014656	0.30865
PNLIPRP3	0.014694	0.308539
SMAD7	0.014717	0.308468
AMMECR1L	0.014735	0.308417
RSPO3	0.014882	0.307985
KCTD9	0.01489	0.307962
HERC4	0.014986	0.307683
ABCA10	0.014992	0.307666
ATP1B3	0.015027	0.307563
GAB1	0.015067	0.307447
ATP8B3	0.015089	0.307384
PURA	0.015185	0.307107
GK5	0.015222	0.307
FLG	0.015312	0.306744

OXR1	0.015348	0.306641
RGS6	0.015435	0.306393
ESCO1	0.015457	0.306331
AP1G1	0.015463	0.306313
ERCC6	0.015469	0.306298
CARD6	0.015471	0.306291
PAQR6	0.015541	0.306094
IGSF3	0.015614	0.305888
EPAS1	0.015656	0.30577
IER5	0.015735	0.30555
ZMYND11	0.015772	0.305447
FAM177A1	0.01588	0.305147
PEX11A	0.015911	0.305063
ZNF319	0.015989	0.304848
S100A7	0.01603	0.304733
SPRR2B	0.01604	0.304706
VCPIP1	0.016145	0.304419
LCE3D	0.016163	0.30437
PAPLN	0.016166	0.304363
HS3ST6	0.016261	0.304104
BLZF1	0.016287	0.304033
NCK1	0.016306	0.303983
STX16	0.016309	0.303975
GAS1	0.016402	0.303725
SRPX2	0.016427	0.303657
UBE2Q2	0.016477	0.303523
GTF3C3	0.016479	0.303518
SCYL2	0.016487	0.303495
ZNF710	0.016538	0.303359
PITPNM3	0.016581	0.303244
RNASEL	0.016645	0.303075
UBXN2A	0.016726	0.30286
TNKS	0.016739	0.302825
ZNF654	0.016754	0.302785
BMP10	0.016802	0.302658
TNFAIP2	0.016819	0.302614
ZDHHC21	0.016834	0.302574
NRBF2	0.016934	0.302313
PI4K2A	0.016988	0.30217
PMS1	0.017038	0.302042
ZBTB43	0.017066	0.301968
A2ML1	0.017125	0.301816
RHOV	0.01719	0.301646
LCE1B	0.017197	0.301628
ASH1L	0.017239	0.30152
CSNK1G1	0.01725	0.301491
OR2G2	0.017301	0.301362
TMCO1	0.017337	0.301267
MLLT10	0.017348	0.301239
CRCP	0.017439	0.301006
KIF16B	0.017454	0.300968
OR52E2	0.017471	0.300927
GTF2IRD1	0.017626	0.300531
HERC3	0.017649	0.300473

ARPP19	0.017828	0.300024